

1 *REVIEW ARTICLE*

2

3 **Hydrogen sulfide signaling in plants**

4

5 Jingjing Huang<sup>1,2</sup> and Yanjie Xie<sup>3</sup>

6

7 <sup>1</sup>Department of Plant Biotechnology and Bioinformatics, Ghent University, 9052 Ghent,  
8 Belgium

9 <sup>2</sup>Center for Plant Systems Biology, VIB, 9052 Ghent, Belgium

10 <sup>3</sup>Laboratory Center of Life Sciences, College of Life Sciences, Nanjing Agricultural University,  
11 Nanjing 210095, PR China

12

13 Corresponding authors:

14 *Jingjing Huang*

15 *Department of Plant Biotechnology and Bioinformatics, Ghent University*

16 *VIB-UGent Center for Plant Systems Biology*

17 *Ghent University*

18 *Technologiepark-Zwijnaarde 71*

19 *9052 Ghent*

20 *Belgium*

21 *E-mail: jingjing.huang@psb.ugent.be*

22 *and*

23 *Yanjie Xie*

24 *Laboratory Center of Life Sciences*

25 *College of Life Sciences*

26 *Nanjing Agricultural University*

27 *address Weigang No.1*

28 *Nanjing 210095*

29 *PR China*

30 *E-mail: yjxie@njau.edu.cn*

31

32 ORCID ID: 0000-0002-4963-3162 (J.H.); 0000-0002-3503-1267 (Y.X.)

33 **Abstract**

34 **Significance:** Hydrogen sulfide (H<sub>2</sub>S) is a multitasking potent regulator that facilitates plant  
35 growth, development, and responses to environmental stimuli.

36 **Recent Advances:** The **important** beneficial effects of H<sub>2</sub>S in various aspects of plant  
37 physiology **aroused** the interest of this chemical for agriculture. Protein cysteine persulfidation  
38 has been recognized as the main redox regulatory mechanism of H<sub>2</sub>S signaling. An increasing  
39 number of studies, including large-scale proteomic analyses and function characterizations,  
40 have revealed that H<sub>2</sub>S-mediated persulfidations directly regulate protein functions, altering  
41 downstream signaling in plants. To date, the importance of H<sub>2</sub>S-mediated persulfidation in  
42 **several abscisic acid signaling-controlling key proteins has been assessed as well as their role**  
43 in stomatal movements, largely contributing to the understanding of the plant H<sub>2</sub>S-regulatory  
44 mechanism.

45 **Critical Issues:** The molecular mechanisms of the H<sub>2</sub>S sensing and transduction in plants  
46 remain elusive. The correlation between H<sub>2</sub>S-mediated persulfidation with other oxidative  
47 posttranslational modifications of cysteines are still to be explored.

48 **Future Directions:** Implementation of advanced detection approaches for the spatiotemporal  
49 monitoring of H<sub>2</sub>S levels in cells and the current proteomic profiling strategies for the  
50 identification and quantification of the cysteine site-specific persulfidation will provide insight  
51 into the H<sub>2</sub>S signaling in plants.

52

53 **Keywords:** hydrogen sulfide, persulfidation, abscisic acid, stomatal movement

54

## 55 Introduction

56

57 Sulfur is the 10th most abundant chemical element in the universe and is essential for all  
58 living organisms (Räisänen, 2005). It occupies a unique position in the reduction–oxidation  
59 (redox) biology due to its availability to reach many distinct oxidation states, ranging from –2  
60 to + 6 (Fig. 1). As the planet got oxidized, sulfate (+6) became the most abundant inorganic  
61 form of sulfur on earth. Hydrogen sulfide (H<sub>2</sub>S), the most reduced inorganic form of sulfur (-2)  
62 (Fig. 1), is a colorless, but flammable, gas, smelling of rotten eggs that is naturally released  
63 from volcanic emissions or other geothermal activities and from decaying plant and animal  
64 proteins.

65 As H<sub>2</sub>S is a weak acid with the dissociation constants  $pK_{a1}$  of 6.9 (Pomeroy, 1941) and  $pK_{a2}$   
66 of between 12 and 17 (Ellis and Golding, 1959, Meyer et al., 1983), it can be dissociated into  
67 hydrosulfide (HS<sup>-</sup>) and sulfide (S<sup>2-</sup>) anions in aqueous solutions. H<sub>2</sub>S usually stands for all  
68 species, including H<sub>2</sub>S, HS<sup>-</sup>, and S<sup>2-</sup> (Paulsen and Carroll, 2013). Nevertheless, in solutions at  
69 an approximately physiological pH of 7.4, H<sub>2</sub>S releases negligible amount of S<sup>2-</sup> and exists  
70 primarily as HS<sup>-</sup> (Hughes et al., 2009). Given the basic chemical properties of H<sub>2</sub>S and HS<sup>-</sup>  
71 with the lowest oxidation state of –2, they both can only be oxidized. Whereas H<sub>2</sub>S is a  
72 gasotransmitter that can diffuse freely across cellular membranes, HS<sup>-</sup> needs specific ion  
73 channels to move between different subcellular organelles or cells (Kabil and Banerjee, 2010).  
74 Accordingly, the H<sub>2</sub>S and HS<sup>-</sup> might regulate cellular functions differently. H<sub>2</sub>S, HS<sup>-</sup>, and S<sup>2-</sup>,  
75 together with various chemically reactive forms of cysteine thiols (see below) and other sulfur-  
76 containing compounds that either reduce or oxidize biomolecules, can be classified as reactive  
77 sulfur species (RSS).

78 H<sub>2</sub>S has been implicated in the origin of life (Filipovic et al., 2018; Olson and Straub, 2016).  
79 Life began 3.8 billion years ago (bya) in a anoxic and ferrous ion (Fe<sup>2+</sup>)-rich ocean.  
80 Cyanobacteria, the first photosynthetic oxygen-generating organisms, are believed to have then  
81 evolved and contributed to the Great Oxygenation Event around 2.5 bya (Demoulin et al., 2019;  
82 Fournier et al., 2021; Planavsky et al., 2014). Along with the slightly increased oxygen level,  
83 sulfur oxidized to sulfate, which was further reduced to sulfide by ubiquitous Fe<sup>2+</sup> present in  
84 the ocean, greatly increasing the H<sub>2</sub>S level and, consequently, leading to a anoxic and sulfidic  
85 ocean (Cortese-Krott et al., 2017). The first eukaryotes appeared and adapted under this  
86 condition using H<sub>2</sub>S as their major energy source (Olson and Straub, 2016). Green algae, one  
87 of the earliest photosynthetic eukaryotes of the Plantae kingdom that contained primary  
88 chloroplasts, derived from endosymbiosis with cyanobacteria, are assumed to have evolved as

89 early as 1.0 bya (Tang et al., 2020). The combined activity of cyanobacteria and algae  
90 tremendously increased the level of ambient oxygen approximately 0.6 bya, sequentially, land  
91 plants have evolved. The antioxidant enzymes, such as superoxide dismutase (Cannio et al.,  
92 2000; Miller, 2012), catalase (Zamocky et al., 2008), glutathione peroxidase (Margis et al.,  
93 2008), peroxiredoxins (Dietz, 2011; Knoops et al., 2007), thioredoxins (TRXs) (Balsera and  
94 Buchanan, 2019), and glutaredoxins (GRXs) (Alves et al., 2009), were already present in an  
95 anoxic and high H<sub>2</sub>S environment as early as 2.0 bya (Cortese-Krott et al., 2017). Therefore,  
96 these redox regulation systems most probably evolved primarily to use H<sub>2</sub>S as energy source or  
97 to deal with RSS, which was later amended to regulate reactive oxygen species (ROS) (Olson  
98 and Straub, 2016; Cortese-Krott et al., 2017). Along with the evolution and increasing  
99 complexity of organisms, the ancient mechanisms of H<sub>2</sub>S metabolism and regulation had to be  
100 adapted. For example, the sulfate transport system in chloroplasts has been suggested to  
101 undergo several adaptations, spanning the evolution of green algae, liverworts, and flowering  
102 plants (Kopriva et al., 2015; Mendoza-Cózatl et al., 2005; Takahashi et al., 2012). In brief, H<sub>2</sub>S  
103 metabolism as well as regulatory mechanisms in living organisms have evolved as the result of  
104 environmental adaptation, while the fundamental principles might remain conserved (Yamasaki  
105 and Cohen, 2016).

106 Besides its implied vital role in evolution, H<sub>2</sub>S has been recognized as a potent signaling  
107 molecule in the regulation of critical cellular processes (Wang, 2002, 2014). Increasing  
108 evidence has shown that H<sub>2</sub>S is not only involved in plant growth, development, reproduction  
109 processes (Baudouin et al., 2016; Chen et al., 2011; Ma et al., 2021), and promotion of  
110 nodulation in the rhizobium-legume symbiosis (Zou et al., 2019), but also facilitates tolerance  
111 to various environmental stresses, such as drought (Jin et al., 2011; Shen et al., 2013), salinity  
112 (Christou et al., 2013; Li et al., 2014a), heavy metals (Fu et al., 2019, Zhang et al., 2020b), and  
113 extreme temperatures (Du et al., 2021; Li et al., 2012). Furthermore, H<sub>2</sub>S has been reported to  
114 improve the quality maintenance during postharvest storage of fruit (Ge et al., 2017; Hu et al.,  
115 2012), vegetables (Li et al., 2014b), and flowers (Zhang et al., 2011). Given the important  
116 beneficial effects of H<sub>2</sub>S in multiple aspects of plant physiology, exogenous H<sub>2</sub>S seems to be a  
117 promising biotechnological strategy with a great agronomic interest.

118 Numerous studies have uncovered the positive physiological impact of H<sub>2</sub>S on plants  
119 (Corpas, 2019; Corpas and Palma, 2020; Zhang et al., 2021), but how plants sense and transduce  
120 H<sub>2</sub>S signals remains elusive. H<sub>2</sub>S can modify proteins through posttranslational modification  
121 (PTM), a process named persulfidation. Persulfidation on critical proteins plays an important  
122 role in activating downstream signaling as demonstrated by both proteomic analyses and

123 functional characterizations (Aroca et al., 2015, 2017b, 2021a, 2021b; Fu et al., 2020a;  
124 Laureano-Marín et al., 2020; Zivanovic et al., 2019). Recently, H<sub>2</sub>S-induced protein  
125 persulfidation has been found to regulate stomatal movements in the abscisic acid (ABA)  
126 signaling pathway (Chen et al., 2020; Shen et al., 2020; Zhou et al., 2021), **contributing to the**  
127 **understanding of the molecular mechanism of H<sub>2</sub>S signaling in plants.**

128 In this review, we provide a wide perspective of H<sub>2</sub>S in plants, including H<sub>2</sub>S biosynthesis,  
129 **exogenous application**, endogenous detection methods, and the mechanisms and identification  
130 strategies for protein persulfidation. We further give insights into the molecular mechanisms of  
131 persulfidation in the regulation of ABA-mediated stomatal closure by highlighting several  
132 recent functional studies.

133

### 134 **H<sub>2</sub>S biosynthesis in plants**

135

136 Plants generate H<sub>2</sub>S endogenously through several biosynthesis pathways in different  
137 subcellular organelles (Fig. 2). The major H<sub>2</sub>S source is associated with the photosynthetic  
138 sulfate assimilation pathway in chloroplasts. **Plants take up sulfate from the environment**  
139 **through sulfate transporters (Takahashi et al., 2011), a protein class with high sulfate affinity**  
140 **that facilitates sulfate trafficking across membranes, into the chloroplasts**, where H<sub>2</sub>S is mainly  
141 generated through sulfur metabolism. Sulfate is reduced by ATP sulfurylase to form the  
142 adenosine 5'-phosphosulfate (APS) intermediate that is further reduced to sulfite by the APS  
143 reductase. H<sub>2</sub>S is then produced from sulfite in the reaction catalyzed by sulfite reductase  
144 (Takahashi et al., 2011) (Fig. 2). H<sub>2</sub>S reacts with *O*-acetylserine (OAS), generating cysteine via  
145 catalyzation by OAS (thiol)lyase (OAS-TL) (Fig. 2). Based on an *in vitro* activity assay, OAS-  
146 TL has been suggested to catalyze the reverse reaction to break down cysteine into H<sub>2</sub>S and  
147 OAS (Burandt et al., 2001). However, negligible **amounts of H<sub>2</sub>S were** formed when compared  
148 to the cysteine production, indicating that the OAS-TL reaction is a net H<sub>2</sub>S-consuming reaction  
149 (Bloem et al., 2004). Moreover, **the production of endogenous H<sub>2</sub>S in planta by OAS-TL**  
150 remains unclear. In plants, the main OAS-TLs responsible for cysteine synthesis are the  
151 cytosolic OAS-TL A1, the chloroplastic OAS-TL B, and the mitochondrial OAS-TL C (Fig. 2).  
152 Recently, the H<sub>2</sub>S level was found to be higher in an *oas-1l a1* mutant than that of wild-type  
153 *Arabidopsis thaliana* plants, confirming the major biological function of OAS-TL in cysteine  
154 biosynthesis rather than in H<sub>2</sub>S generation (Li et al., 2018).

155 Cysteine desulphydrase (CDEs) was the first **studied** H<sub>2</sub>S-producing enzyme (Harrington and  
156 Smith, 1980; Tishel and Mazelis, 1966). Because of its ubiquitous activity in various

157 physiological processes of different plant species (Zhao et al., 2020), CDes is considered to be  
158 the most critical enzymatic source of H<sub>2</sub>S in plants. There are two type of CDes: L-CDes that  
159 degrades L-cysteine and D-CDes that uses D-cysteine as substrate. In the cytosol, L/D-cysteine  
160 is catalyzed by L/D-CDes to produce H<sub>2</sub>S, NH<sub>3</sub>, and pyruvate (Fig. 2). L-CDes 1 (DES1), an  
161 OAS-TL homolog located in the cytosol, had originally been thought to have a function similar  
162 to that of OAS-TL A1, until its CDes activity had been proven (Álvarez et al., 2010). The  
163 *Arabidopsis DES1* gene is ubiquitously expressed at all developmental stages in plants  
164 (Laureano-Marín et al., 2014) and its function has been extensively investigated in the context  
165 of H<sub>2</sub>S signaling in ABA-mediated stomatal movement (see below). Moreover, the nitrogenase  
166 Fe–S cluster (NifS), localized both in chloroplasts and mitochondria, is also a putative H<sub>2</sub>S-  
167 producing enzyme due to its L-CDes-like activity (Pilon-Smits et al., 2002; Van Hoewyk et al.,  
168 2008). In addition, the mitochondrial β-cyanoalanine synthase (CAS) detoxifies cyanide that  
169 appeared in the cells to β-cyanoalanine in the presence of cysteine, along with the production  
170 of H<sub>2</sub>S (Hatzfeld et al., 2000) (Fig. 2).

171 In mammals, 3-mercaptopyruvate sulfurtransferase (MST) that belongs to the  
172 sulfurtransferase (STR) family, is one of the **most important** H<sub>2</sub>S-producing enzymes, but  
173 information about MST in plants is scarce. Recently, two *Arabidopsis* MSTs, the mitochondrial  
174 STR1 and the cytosolic STR2, were characterized by means of an *in vitro* activity assay,  
175 revealing their H<sub>2</sub>S-producing capability in the presence of reducing systems, such as **TRXs**  
176 **and GRXs** (Moseler et al., 2021). Nevertheless, the *in planta* contribution to H<sub>2</sub>S biosynthesis  
177 from STR1 and STR2 awaits to be further investigated.

178

## 179 **Exogenous H<sub>2</sub>S application in plants**

180

181 **Currently, investigation of the physiological roles of H<sub>2</sub>S is mainly based on studies applying**  
182 **exogenous H<sub>2</sub>S donors. To date, various H<sub>2</sub>S donors have been developed (Powell et al., 2018;**  
183 **Yang et al., 2022) and have been widely used in plant studies (Corpas, 2019; Corpas and Palma,**  
184 **2020; Liu et al., 2021). Here we provide a short discussion and an update on the these donors.**

185 **Sulfide salts, such as sodium hydrosulfide (NaHS) and sodium sulfide (Na<sub>2</sub>S), are inorganic**  
186 **compounds that release H<sub>2</sub>S by hydrolysis. To date, NaHS is the most popular and widely**  
187 **applied H<sub>2</sub>S donor in various plant species (Corpas, 2019; Corpas and Palma, 2020; Liu et al.,**  
188 **2021). The use of NaHS as H<sub>2</sub>S donor has greatly improved our understanding of the biological**  
189 **function of H<sub>2</sub>S, but the NaHS shortcoming is that it does not mimic the biological effects of**  
190 **the physiological H<sub>2</sub>S generation. Indeed, NaHS hydrolyzes immediately in aqueous solutions**

191 and instantaneously releases large amount of H<sub>2</sub>S, HS<sup>-</sup>, and S<sup>2-</sup> species, a process very different  
192 from the endogenously slow and continuous H<sub>2</sub>S enzymatic production. Therefore, chemicals  
193 with a slow H<sub>2</sub>S-releasing rate are required.

194 The morpholin-4-ium 4-methoxyphenyl(morpholino) phosphinodithioate (GYY4137) is  
195 such a slow releasing H<sub>2</sub>S compound that had initially been synthesized and evaluated with a  
196 vasodilatorory and antihypertensive activity (Li et al., 2008). Due to the commercial availability  
197 and application feasibility, GYY4137 is the most widely used H<sub>2</sub>S donor, besides from sulfide  
198 salts in the mammalian field (Powell et al., 2018). In plants, GYY4137 often applied in parallel  
199 with NaHS that has similar effects. For example, similarly to NaHS, GYY4137 application  
200 could induce stomata closure in *Arabidopsis* (García-Mata and Lamattina, 2010; Honda et al.,  
201 2015) and *Nicotiana tabacum* (tobacco) (Papanatsiou et al., 2015) and could improve growth  
202 of *Pisum sativum* (pea), *Lactuca sativa* (lettuce), and *Raphanus sativa* (radish) (Carter et al.,  
203 2018).

204 Recent environmentally friendly slow H<sub>2</sub>S-releasing chemicals, dialkyldithiophosphates and  
205 disulfidedithiophosphates, have been shown to improve the growth of *Zea mays* (maize) plants,  
206 hinting at potential applicability in agriculture (Brown et al., 2021; Carter et al., 2019). Another  
207 novel H<sub>2</sub>S donor is a class of nitric oxide (NO)–hydrogen sulfide-releasing hybrid (NOSH)  
208 compounds that release NO and H<sub>2</sub>S simultaneously, which was designed for its extreme  
209 effectiveness in growth inhibition of human cancer cell lines (Kodela et al., 2012). NOSH and  
210 its aspirin hybrid (NOSH-aspirin) that additionally releases acetylsalicylic acid have been  
211 shown to improve drought tolerance of *Medicago sativa* (alfalfa) (Antoniou et al., 2020),  
212 suggesting NOSH might be a promising plant priming agent against environmental stresses.

213 H<sub>2</sub>S has been reported to act as electron donor for respiration and to contribute to ATP  
214 production in mitochondria of prokaryotes (Sakurai et al., 2010) and in a variety of species,  
215 such as California killifish (*Fundulus parvipinnis*) (Bagarinao and Vetter, 1990), marine mussel  
216 (*Geukensia demissa*) (Doeller et al., 1999, 2001; Parrino et al., 2000), sandworm (*Arenicola*  
217 *marina*) (Vökel and Grieshaber, 1997), chicken (*Gallus gallus*) (Yong and Searcy, 2001), and  
218 human (*Homo sapiens*) (Goubern et al., 2007). A mitochondria-specific H<sub>2</sub>S donor, (10-oxo-  
219 10-(4-(3-thioxo-3H-1,2-dithiol-5yl)phenoxy)decyl) triphenylphosphonium bromide (AP39)  
220 (Le Trionnaire et al., 2014) can be used as a useful tool to specifically investigate the biological  
221 function of H<sub>2</sub>S in mitochondria. AP39 was initially used in murine microvascular endothelial  
222 cells, had an antioxidant and cytoprotective impact under oxidative stress conditions (Szczeny  
223 et al., 2014), and later improved the mitochondrial function in the nematode *Caenorhabditis*  
224 *elegans* (Fox et al., 2021). H<sub>2</sub>S is certainly tightly linked to the mitochondrial electron transport

225 chain (ETC) activity in the above mentioned species. However, the knowledge of this aspect in  
226 plants remains modest. Recently, AP39 was applied in *Arabidopsis* to investigate stomata  
227 movement (Pantaleo et al., 2023). In addition to the induction of stomatal closure, AP39 could  
228 modulate mitochondrial ETC activity and redox homeostasis of guard cells, providing the first  
229 piece of evidence that H<sub>2</sub>S modulates mitochondrial energetics in plants.

230

### 231 ***In vivo* detection of H<sub>2</sub>S in plants**

232

233 The important physiological functions of H<sub>2</sub>S have attracted attention in plant research,  
234 compelling the development of detection techniques in living cells, tissues, and different  
235 organisms, but the direct detection of endogenous H<sub>2</sub>S in plants remains a challenge. Traditional  
236 detection methods for H<sub>2</sub>S, such as colorimetric assays (Siegel, 1965), gas chromatography  
237 (Hannestad et al., 1989), high-performance liquid chromatography (Shen et al., 2011),  
238 polarographic H<sub>2</sub>S sensor (Doeller et al., 2005), and ion-selective electrode (ISE) (Li et al.,  
239 2000), typically require sample destruction and are limited to *in vitro* detection. Fluorescent  
240 probes are emerging as tools for the noninvasive study of reactive species *in situ* in different  
241 biological systems, because of their high cell permeability and specificity. Different fluorescent  
242 approaches, including chemical and genetically encoded probes, have been used for H<sub>2</sub>S  
243 detection (Chen et al., 2012; Chen et al., 2013b; Lin et al., 2015; Liu et al., 2011a; Youssef et  
244 al., 2019). Despite the considerably fewer reports in plants than in the mammalian field,  
245 fluorescent probes are considered effective and noninvasive tools for the real-time detection  
246 and imaging of H<sub>2</sub>S in plants.

247 As the methods for H<sub>2</sub>S detection have been extensively reviewed (Filipovic et al., 2018;  
248 Kong et al., 2022; Lin et al., 2015; Luo et al., 2022; Zeng et al., 2021; Zhao et al., 2020), we  
249 will discuss the fluorescent probes recently used to discover endogenous H<sub>2</sub>S in different plant  
250 species and organisms. In general, the various strategies can be categorized in three groups  
251 based on the reaction types, namely azide/nitro/nitroso reduction, copper sulfide precipitation,  
252 and nucleophilic reaction-based methods (Luo et al., 2022). The fluorescent probes used in  
253 plant studies are mainly based on azide reduction and nucleophilic reaction (Fig. 3).

254

#### 255 *AzMC*

256

257 The azide reduction-based chemical probe, 7-azido-4-methylcoumarin (AzMC), is  
258 commercially available. The strong electron-withdrawing ability of the azide group of AzMC

259 quenches its fluorescence, whereas H<sub>2</sub>S reduces the azide to amine, thus turning on the  
260 fluorescence (Kong et al., 2022). Initially, AzMC has been used in photoaffinity labeling of the  
261 substrate-binding site of the human phenol sulfotransferase (Chen et al., 1999) and later for H<sub>2</sub>S  
262 detection in living cells and cardiac tissues (Chen et al., 2013a). In plants, AzMC was first  
263 applied to measure the H<sub>2</sub>S level in tomato (*Solanum lycopersicum*) guard cells in response to  
264 ethylene signal transduction upon osmotic stress (Jia et al., 2018), Recently, this probe has been  
265 utilized to determine H<sub>2</sub>S levels in *Arabidopsis* guard cells from wild-type and *des1* mutant  
266 plants, **which are deficient in cytosolic H<sub>2</sub>S generation due to the lack of DES1**, in response of  
267 ABA-induced--stomatal closure (Shen et al., 2020; Zhang et al., 2020a). The ABA-induced H<sub>2</sub>S  
268 accumulation in guard cells of wild-type plants was abolished in the *des1* mutant plants,  
269 whereas the H<sub>2</sub>S donor NaHS could clearly induce H<sub>2</sub>S in plants of both genotypes (Fig. 3),  
270 **indicating that DES1 is responsible for the sensitivity of ABA-induced stomatal closure (Zhang**  
271 **et al., 2020a).**

272

273 *SiND-ANPA-N<sub>3</sub>*

274

275 Another azide reduction-based chemical probe is the silicon nanodots-4-azido-N-alanine-1,8-  
276 naphthalimide (SiND-ANPA-N<sub>3</sub>). This probe contains three moieties, the two-photon  
277 fluorophore dye *N*-alanine-1,8-naphthalimide, the azido adduct responsible for reduction-  
278 activated fluorescence, and the attached silicon nanodot (SiND) that increases water solubility  
279 and cell permeability. This probe has been tested in the inner-layer epidermal tissues of onion  
280 (*Allium cepa*) and evaluated as a potential probe for H<sub>2</sub>S detection in aqueous media and living  
281 cells (Fu et al., 2020b) (Fig. 3).

282

283 *WSP-1*

284

285 The Washington state probe-1 (WSP-1) is a nucleophilic reaction-based chemical probe (Liu  
286 et al., 2011a) that contains a pyridyl disulfide moiety and a fluorophore group. H<sub>2</sub>S reacts with  
287 the pyridyl disulfide and generates a persulfide intermediate that undergoes a spontaneous  
288 intramolecular cyclization to release the fluorophore. **By using WSP-1 in tomato roots, an**  
289 **increased level of H<sub>2</sub>S was detected upon an exogenous NO donor treatment, which was**  
290 **inhibited by applying the NO scavenger cPTIO (Li et al., 2014c) (Fig. 3).** Until now, WSP-1  
291 was utilized for endogenous H<sub>2</sub>S detection in the roots of turnip (*Brassica rapa*) and the H<sub>2</sub>S  
292 level decreased upon selenium treatment (Chen et al., 2014) (Fig. 3).

293

294 *SSP4*

295

296 The nucleophilic reaction-based sulfane sulfur probe, sulfane sulfur probe 4 (SSP4), has been  
297 developed based on the original design of the SSP1 and SSP2 probes (Chen et al., 2013b).  
298 Sulfane sulfur reacts with the nucleophilic thiols in the nonfluorescent SSP4 to form a persulfide  
299 intermediate that reacts with electrophilic ester groups, leading to spontaneous intramolecular  
300 cyclization and release of the fluorophore. Recently, SSP4 has been used for endogenous H<sub>2</sub>S  
301 detection during the root nodule symbiosis in the legume *Lotus japonicus* and an increased level  
302 of H<sub>2</sub>S has been observed during nodulation (Fukudome et al., 2020) (Fig. 3). SSP4 is  
303 commercially available and has a relatively high selectivity and sensitivity to sulfane sulfurs.  
304 However, sulfane sulfur probes are not specific for H<sub>2</sub>S, because they also react with persulfides  
305 and polysulfides.

306

307 *SSNIP*

308

309 Another sulfane sulfur probe that shares a thiophenol moiety and an ester linker with the **SSP4**  
310 **probe is attached to a near-infrared (NIR) fluorophore, designated sulfane sulfur NIR probe**  
311 **(SSNIP)**. The SSNIP probe has been tested in *Arabidopsis* roots (Fig. 3) during different growth  
312 stages (Jiang et al., 2019).

313

314 *HBTP-H<sub>2</sub>S*

315

316 The 2-(2-hydroxyphenyl) benzothiazole-based H<sub>2</sub>S probe, HBTP-H<sub>2</sub>S, is a recent NIR  
317 fluorescent probe and contains a dinitrophenyl (DNP) ether that undergoes thiolysis under  
318 nucleophilic attacks by H<sub>2</sub>S, releasing the fluorophore. This NIR fluorescent probe has been  
319 applied for *in situ* bioimaging of endogenous H<sub>2</sub>S in rice (*Oryza sativa*) roots and revealed an  
320 increased level of H<sub>2</sub>S under Al<sup>3+</sup> and flooding stresses (Wang et al., 2021) (Fig. 3).

321

322 *Genetically encoded H<sub>2</sub>S sensors*

323

324 Since 2012, reaction-based genetically encoded fluorescent H<sub>2</sub>S sensors have been studied  
325 and a probe based on *p*-azidophenylalanine (pAzF) was originally developed and tested by  
326 expressing the cpGFP-Tyr66pAzF in HeLa cells (Chen et al., 2012). This pAzF-based genetic

327 probe has been optimized by modification with pAzF of the chromophore of a circularly  
328 permuted, superfolder green fluorescent protein (cpsGFP) to derive the cpsGFP-pAzF, which  
329 subsequently served as a Förster resonance energy transfer acceptor to an enhanced blue  
330 fluorescent protein EBFP2 (Youssef et al., 2019). Thus far, the H<sub>2</sub>S genetic probe has not been  
331 utilized in plant research, whereas other genetic sensors, such as HyPer or the roGFP series for  
332 hydrogen peroxide (H<sub>2</sub>O<sub>2</sub>) sensing, and SoNar or Peroxox for NADH/NAD<sup>+</sup> sensing (Müller-  
333 Schüssele et al., 2021), have been extensively used for monitoring the redox states in living  
334 plant cells. The development or application of genetic probes for real-time H<sub>2</sub>S monitoring in  
335 plant research would be greatly beneficial for understanding the H<sub>2</sub>S-regulatory mechanisms in  
336 plants.

337

### 338 H<sub>2</sub>S signaling via protein persulfidation

339

340 Protein persulfidation, also called S-sulfhydration, as a type of oxidative PTM of cysteines,  
341 has been increasingly recognized as the main redox mechanism directly regulating diverse  
342 biological processes in H<sub>2</sub>S signaling, such as protein function, structure, and subcellular  
343 localization. Protein cysteine thiols (–SH) are very susceptible to H<sub>2</sub>O<sub>2</sub> and can undergo  
344 different oxidative PTMs. Initially, thiol reacts with H<sub>2</sub>O<sub>2</sub> to form sulfenic acid (–SOH) (Allison,  
345 1976) that is intrinsically unstable and an intermediary *en route* to other PTMs. In the presence  
346 of H<sub>2</sub>O<sub>2</sub> excess, –SOH forms the relatively more stable sulfinic acid (–SO<sub>2</sub>H) and sulfonic acid  
347 (–SO<sub>3</sub>H) (Cremllyn, 1996), which are generally considered to cause protein overoxidation (Fig.  
348 4). The –SO<sub>3</sub>H formation is irreversible, whereas –SO<sub>2</sub>H can be reduced via an ATP-dependent  
349 reaction by sulfiredoxin of certain proteins (Akter et al., 2018; Biteau et al., 2003). Alternatively,  
350 –SOH can react with proximal –SHs from proteins and with glutathione (GSH), forming  
351 intra/intermolecular disulfide (–SS–) (Nagy and Winterbourn, 2010, Turell et al., 2021) and S-  
352 glutathione adduct (–SSG) (Turell et al., 2008), respectively (Fig. 4). Disulfides and glutathione  
353 adducts can be enzymatically reduced to –SH by thiol reductases, so-called redoxins, such as  
354 TRXs and GRXs (Huang et al., 2018; Willems et al., 2021). Besides H<sub>2</sub>O<sub>2</sub>, reactive nitrogen  
355 species, which mainly refer to NO, trigger the formation of S-nitrosothiols (–SNO) (Hess et al.,  
356 2005) that can also be reduced by redoxins.

357 H<sub>2</sub>S reacts with oxidized, not reduced, thiols, –SOH, and disulfides specifically, to form  
358 persulfides (–SSH) (Cuevasanta et al., 2015). The kinetics of the H<sub>2</sub>S reactions with low-  
359 molecular weight albumin disulfides and –SOH have been determined. The rate constant of H<sub>2</sub>S  
360 with –SOH for the formation of persulfides is 270 M<sup>-1</sup>s<sup>-1</sup>, significantly higher than that of

361 disulfides ( $0.6 \text{ M}^{-1}\text{s}^{-1}$ ), implying that the formation of protein persulfides might mainly occur  
362 through reaction of  $\text{H}_2\text{S}$  with  $-\text{SOH}$ . However, extremely high reaction rates of protein  
363 disulfides with  $\text{H}_2\text{S}$  have been detected in some special cases, such as human sulfide quinone  
364 oxidoreductase (Cuevasanta et al., 2017). Furthermore, protein disulfides are relatively more  
365 stable than the labile  $-\text{SOH}$  in the environment; hence, the generation of protein persulfides via  
366 the  $\text{H}_2\text{S}$  reaction with disulfides cannot be excluded. Persulfides might be formed by reaction  
367 of  $\text{H}_2\text{S}$  with  $-\text{SNO}$  or  $-\text{SSG}$  (Francoleon et al., 2011; Iciek et al., 2015; Mishanina et al., 2015),  
368 but this reaction mainly remains hypothetical and needs further investigation.

369 Protein persulfides can be oxidized by  $\text{H}_2\text{O}_2$  to form perthiosulfenic acid ( $-\text{SSOH}$ ),  
370 perthiosulfenic acid ( $-\text{SSO}_2\text{H}$ ), and perthiosulfonic acid ( $-\text{SSO}_3\text{H}$ ). In contrast to the hardly  
371 reversible  $-\text{SO}_2\text{H}$  and irreversible  $-\text{SO}_3\text{H}$  formed upon  $\text{H}_2\text{O}_2$  overoxidation, the corresponding  
372  $-\text{SSH}$  and its oxidative derivatives can be reduced by redoxins (Dóka et al., 2020; Filipovic,  
373 2015; Ju et al., 2016; Wedmann et al., 2016) (Fig. 4).

374

### 375 **Protein persulfidation detection in plants**

376

377 In the past decade, a variety of detection methods for efficient persulfidation labeling and  
378 identification have been developed **to investigate the  $\text{H}_2\text{S}$  signaling executed via persulfidation.**  
379 Protein persulfidation can be directly detected by means of mass spectrometry (MS), because  
380 of the mass increase of 31.972 Da by the addition of one sulfur atom, but is difficult to  
381 distinguish from other modification, such as  $-\text{SO}_2\text{H}$  due to the addition of two oxygen atoms  
382 (mass increase of 31.99 Da). Thus, specific labeling with chemical probes is required to  
383 **persulfidation detection.** Initially, a modified biotin switch method had been applied in human  
384 cells, in which methyl methanethiosulfonate (MMTS) was believed to specifically block  $-\text{SH}$ ,  
385 whereafter  $-\text{SSH}$  was targeted and enriched with *N*-[6-(biotinamido) hexyl]-3'-(2'-  
386 pyridyldithio)propionamide (biotin-HPDP) (Mustafa et al., 2009). In plants, this method was  
387 first utilized in *Arabidopsis* leaf extracts **and 106 persulfided proteins were identified** (Aroca et  
388 al., 2015). However, because the reactivity toward MMTS of SSH **was higher than** that of thiols  
389 (Pan and Carroll, 2013), this method was questioned and should be used with caution.

390 The most challenging aspect of persulfidation detection is the discriminative labeling from  
391 thiols, because of their similar reactivity to commonly used reagents through alkylation, such  
392 as maleimide, *N*-ethylmaleimide (NEM), and iodoacetamide (IAM) (Pan and Carroll, 2013).  
393 Due to their greater nucleophilicity, persulfides react even much faster than thiols to thiol  
394 labeling reagents (Cuevasanta et al., 2015). Nevertheless, because alkylation of thiols yield

395 thioethers, whereas persulfides generate disulfides, many thiol label-based detection  
396 approaches have been exploited based on this characteristic.

397 At first, a fluorescent probe, designated red maleimide, had been used to study the  
398 persulfidation of the p65 subunit of **mice** NF- $\kappa$ B (Sen et al., 2012). Both –SH and –SSH are  
399 labeled with red maleimide and followed with dithiothreitol (DTT) reduction, so that only the  
400 labeled –SSH, namely the R–S–S–maleimide-red adducts, are reduced (Fig. 5A). The protein  
401 samples are subsequently separated by gel electrophoresis and detected by in-gel fluorescence.  
402 The loss of fluorescence can be calculated for evaluation of the persulfidation level. This  
403 method revealed the persulfidation of recombinant human glyceraldehyde-3-phosphate  
404 dehydrogenase (GAPDH) protein at Cys150, which enhances its catalytic activity (Gao et al.,  
405 2015).

406 Later, another thiol label-based probe, a maleimide compound containing a peptide arm,  
407 designated maleimide peptide (MalP, 1.95 kDa), was used to study the persulfidation of the  
408 iron-sulfur cluster machinery **in mammalian proteins** (Parent et al., 2015). Similarly as with the  
409 red maleimide fluorescent probe, both –SH and –SSH **are** labeled with MalP and only the  
410 labeled –SSHs **are** further reduced by the subsequent DTT incubation and **release** the  
411 succinimide-peptide moiety (the product of the maleimide reaction with a sulfhydryl). As a  
412 result, the mobility shift in the protein migration can be detected by sodium dodecyl sulfate-  
413 polyacrylamide gel electrophoresis (SDS-PAGE) (Fig. 5A).

414 The two aforementioned approaches offered many advantages, such as relative application  
415 simplicity and radiometric read outs (–SSH versus –SH) giving extra quantification  
416 information. Nevertheless, these method are restricted to biochemical characterizations and are  
417 rather not applicable to large-scale MS-based proteomic analyses.

418 A MS-coupled thiol labeling-based proteomic approach, termed biotin thiol assay (BTA),  
419 had initially been utilized for mapping protein persulfidation in mammalian cells by means of  
420 maleimide-biotin (Cuevasanta et al., 2015), maleimide-PEG2-biotin (Gao et al., 2015), or  
421 iodoacetyl-PEG2-biotin (Dóka et al., 2016, 2019). In this method, –SH and –SSH are first  
422 labeled with biotin-tagged alkylating reagents **that are sequentially enriched on an avidin**  
423 **column, whereafter the labeled –SSHs are selectively eluted by reduction via DTT or tris(2-**  
424 **carboxyethyl)phosphine** (Fig. 5B). By labeling the eluted persulfide-derived thiols by isotope-  
425 labeled (D5, heavy) or normal (H5, light) maleimide, a quantitative analysis under different  
426 conditions **could be achieved** (Gao et al., 2015). Recently, a BTA assay combined with the  
427 iodoacetyl isobaric tandem mass tag system allowed the quantitative cysteine site-specific  
428 identification of persulfidation (Gao et al., 2020).

429 Additionally, a ‘tag-switch’ method was developed for persulfidation detection (Zhang et  
430 al., 2014). Here, methylsulfonyl benzothiazole (MSBT) was used to block both –SH and –SSH,  
431 whereafter solely MSBT disulfide adducts (–SS–MSBT) could react with cyanoacetate biotin  
432 (CN-biotin), hence designated ‘tag switch’ (Fig. 5C). This method was further improved by  
433 attaching cyanoacetate with the fluorescent BODIPY moiety (CN-BOT) or the Cy3 dye (CN-  
434 Cy3), so that persulfidation could be visualized *in situ* by fluorescence confocal microscopy or  
435 in-gel fluorescent detection from the cell lysates (Kouroussis et al., 2019; Wedmann et al.,  
436 2016). In plants, the ‘tag switch’ method was applied in wild-type and *des1* mutant *Arabidopsis*  
437 plants (Aroca et al., 2017a). In total, 2,015 and 2,130 persulfidated proteins were identified in  
438 the wild-type and *des1* plants, respectively, suggesting that a large fraction of the *Arabidopsis*  
439 proteome undergoes persulfidation even under nonstressed conditions (Aroca et al., 2017a).  
440 Recently, the application of the ‘tag switch’ method on *Arabidopsis* root tissue identified 5,214  
441 –SSH proteins (Jurado-Flores et al., 2021).

442 A variant of this tag-switch method for the –SSH identification is called the ‘dimedone  
443 switch’ assay (Zivanovic et al., 2019) (Fig. 5C). In this assay, –SSH, –SH, and –SOH first react  
444 with 4-chloro-7-nitrobenzofurazan (NBF-Cl), whereafter a dimedone-based probe, such as a  
445 biotin-conjugated analog DCP-Bio1 (Poole et al., 2007) or azide-conjugated analog DCP-N<sub>3</sub>,  
446 selectively switches with –SS–NBF disulfides. The biotin-tagged persulfides are subsequently  
447 enriched and identified by MS and by in-gel fluorescence or confocal microscopy when DCP-  
448 Bio1 and DCP-N<sub>3</sub> and Cy5-alkyne click mix are used, respectively (Zivanovic et al., 2019).  
449 This dimedone switch method recently applied in *Arabidopsis* revealed persulfidation of Cys103  
450 of the autophagy-related protein 18a, thereby activating its phospholipid-binding activity in a  
451 reversible manner and, hence, regulating autophagy under endoplasmic reticulum stress (Aroca  
452 et al., 2021a).

453 Currently, a direct persulfidation detection method was developed for proteomic analysis by  
454 labeling –SSH at pH 5.0 by means of an alkyne-linked IAM, *N*-propynyliodoacetamide (IPM)  
455 (Fu et al., 2020a) (Fig. 5D). Given the lower *pK<sub>a</sub>* of persulfide (4.3) than that of thiol (8.29),  
456 persulfides maintain a relatively high reactivity at pH 5.0 when compared to protonated thiols.  
457 Hence, efficient labeling of –SSH can be achieved by labeling proteome extracts with IPM at a  
458 low pH, resulting in disulfide adducts (SS-IPM), in addition to thioether adducts (S-IPM) due  
459 to the unavoidable –SH labeling. IPM-labeled peptides are further biotinylated by reaction with  
460 Az-UV-biotin reagents through a click reaction, the addition of biotin facilitating peptide  
461 enrichment. Two types of probe-modified peptides, including the disulfide forms derived from  
462 –SSH and the thioether forms derived from –SH, can be analyzed by MS (Fu et al., 2020a).

463

## 464 **H<sub>2</sub>S-mediated persulfidation in ABA-regulated stomatal movement**

465

466 Stomata are pores on the epidermis of plant leaves surrounded by a pair of guard cells.  
467 Stomatal movement regulates gas and water exchange between the plants and the environment  
468 and is important for plant growth, development, and response to environmental stimuli (Kim et  
469 al., 2010). That H<sub>2</sub>S induced stomatal closure and participated in ABA signaling was first  
470 evidenced by application of NaHS in epidermal strips of *Vicia faba* (broad bean), *Arabidopsis*  
471 *thaliana* and *Impatiens walleriana* (impatiens) (García-Mata and Lamattina, 2010). In contrast,  
472 H<sub>2</sub>S was reported to cause stomatal opening in *Arabidopsis* (Lisjak et al., 2010) and pepper  
473 (*Capsicum annuum*) (Lisjak et al., 2011). The reason of the opposite effects of H<sub>2</sub>S on stomata  
474 movement remains inconclusive. However, an increasing number of studies subsequently  
475 revealed that H<sub>2</sub>S is a key regulator of stomatal closure triggered by different environmental  
476 stresses, such as drought (Jin et al., 2017), cold (Du et al., 2019), and mediated by  
477 phytohormones, such as ABA that accumulates under drought stress (Jin et al., 2013), ethylene  
478 (ET) (Hou et al., 2016; Liu et al., 2011b), salicylic acid (SA) (He et al., 2020), and jasmonic  
479 acid (JA) (Deng et al., 2020) (Fig. 6). To date, the H<sub>2</sub>S signaling function has been best  
480 characterized in the ABA-regulated stomatal movement. ABA has been generally recognized  
481 as eliciting the *DES1* expression in guard cells that increases the endogenous level of H<sub>2</sub>S,  
482 because DES1-mediated H<sub>2</sub>S production is required for downstream NO signaling (Scuffi et  
483 al., 2014) and respiratory burst oxidase homolog (RBOH)-dependent H<sub>2</sub>O<sub>2</sub> signaling (Scuffi et  
484 al., 2018) to activate stomatal closure (Fig. 6). Besides DES1 and RBOH (Shen et al., 2020),  
485 ABSCISIC ACID INSENSITIVE 4 (ABI4) (Zhou et al., 2020), and SNF1-RELATED  
486 PROTEIN KINASE2.6 (SnRK2.6), also known as Open stomata 1 (OST1) (Chen et al., 2020),  
487 have also been found as key proteins involved in H<sub>2</sub>S signaling in ABA-regulated stomatal  
488 movement (see below). In addition, by means of pharmacological and genetic approaches,  
489 phospholipase D and mitogen-activated protein kinase 4 were shown to participate in H<sub>2</sub>S-  
490 mediated guard cell signaling (Scuffi et al., 2018) and to be an important downstream signal of  
491 H<sub>2</sub>S in stomatal movement in response to drought stress, respectively (Du et al., 2019).

492 Persulfidation on several key proteins in plants have been characterized, such as the critical  
493 antioxidant enzyme ascorbate peroxidase 1 (Aroca et al., 2015), the moonlighting cytosolic  
494 GAPDH protein (Aroca et al., 2017b), the autophagy-related protein 4 (Laureano-Marín et al.,  
495 2020) and 18 (Aroca et al., 2021a). For a recent review, see Aroca et al. (2021b). Here, we focus

496 on the most recent proteins, *i.e.*, DES1, RBOHD, OST1, and ABI4, that are involved in H<sub>2</sub>S  
497 signaling in ABA-regulated stomatal closure (Fig. 7).

498 The ABA level in guard cells under normal conditions remains low, but increases upon stress  
499 stimuli. When ABA is absent, the protein phosphatase type 2C (PP2C) binds to the SnRK2.6  
500 kinase domain and inhibits the kinase activity by dephosphorylation. In the presence of ABA,  
501 it binds to the ABA receptor PYRABACTIN RESISTANCE/PYR-LIKE/REGULATORY  
502 COMPONENT OF ABA RECEPTOR (PYR/PYL/RCAR) to form a complex that binds to  
503 PP2C and inhibits the catalytic activity of PP2C (Fig. 7), **thereby** activating SnRK2.6 because  
504 of its dissociation from PP2C and autophosphorylation (Soon et al., 2012). The activated  
505 SnRK2.6 then transmits the ABA signal by phosphorylating downstream factors, such as  
506 RBOH, ultimately inducing rapid ROS production and cellular Ca<sup>2+</sup> influx and activating  
507 specific ion channels that trigger stomatal closure (Fig. 7).

508 ABA induces the *DES1* expression transcriptionally through an unclear mechanism, thereby  
509 inducing the H<sub>2</sub>S production in guard cells (Scuffi et al., 2014). The ABA-induced H<sub>2</sub>S  
510 production results in the persulfidation of SnRK2.6 at Cys131 and Cys137, which are adjacent  
511 to the catalytic loop of the kinase and the pivotal phosphorylation site Ser175 (Chen et al., 2020)  
512 (Fig. 7). Persulfidation of SnRK2.6 promotes its activity and interacts with the transcription  
513 factor ABA response element-binding factor 2 (ABF2) that enhances the cytosolic Ca<sup>2+</sup>  
514 signaling. Persulfidation of SnRK2.6 at Cys131 and Cys137 alters its protein structure, hence  
515 bringing the Ser175 residue closer to the phosphate-acceptor Asp140 and improving its activity  
516 (Chen et al., 2021). **In contrast, NO negatively regulates ABA signaling in guard cells by**  
517 **inhibiting SnRK2.6 through formation of -SNO at Cys137 (Wang et al., 2015).**

518 SnRK2 phosphorylates the downstream transcription factor Related to ABI3/VP1-Like 1  
519 (RAV1) to inhibit the expression of ABI4 (Feng et al., 2014). ABI4 has been considered as a  
520 versatile activator or repressor of its downstream target genes (Wind et al., 2013). The DES1-  
521 mediated H<sub>2</sub>S production has been reported to induce the persulfidation of ABI4 at Cys250,  
522 which is essential for the ABI4 function in the regulation of plant responses to ABA (Zhou et  
523 al., 2021). The persulfidation of ABI4 at Cys250 enhances its transactivation activity on  
524 **Mitogen-Activated Protein Kinase Kinase Kinase 18 (MAPKKK18)**, thereby activating a  
525 MAPK cascade (Fig. 7). Furthermore, transactivation of *DES1* could be mediated by ABI4  
526 persulfidation, hinting at the existence of a regulatory loop.

527 In addition, we recently demonstrated that H<sub>2</sub>S-mediated persulfidation is involved in ABA  
528 signaling in guard cells by directly regulating the activity of both ROS and H<sub>2</sub>S-producing  
529 enzymes (Shen et al., 2020). Upon ABA treatment, DES1-mediated H<sub>2</sub>S triggers its

530 autopersulfidation at Cys44 and Cys205, leading to a burst of H<sub>2</sub>S in guard cells. The  
531 accumulation of H<sub>2</sub>S further induces the persulfidation of RBOHD Cys825 and Cys890,  
532 enhancing the RBOHD activity and leading to ROS overproduction (Fig. 7). **NO was**  
533 **demonstrated to negatively regulate *Arabidopsis* RBOHD by forming -SNO at Cys 890 during**  
534 **the hypersensitive response in plant immunity (Yun et al., 2011). Nevertheless, NO-mediated**  
535 **modifications on RBOHD still need to be investigated regarding the impact on the ABA**  
536 **signaling in guard cells. Here, the interplays between H<sub>2</sub>S, ROS, and NO involved in the**  
537 **regulatory ABA signaling mechanism in guard cells occur most probably through redox PTMs**  
538 **of key proteins.**

539

## 540 **Summary and Perspectives**

541

542 In the past decades, **numerous** studies revealed the multitasking capacity of H<sub>2</sub>S that is  
543 involved in many physiological and pathological processes in mammals (Dilek et al., 2020;  
544 Kimura et al., 2012; Murphy et al., 2019; Shatalin et al., 2011) and growth, development, and  
545 response to environmental stimuli in plants (Baudouin et al., 2016; Chen et al., 2011; Jin et al.,  
546 2013, 2017; Li et al., 2014a; Zou et al., 2019). Nevertheless, our current knowledge on the  
547 molecular mechanisms by which H<sub>2</sub>S executes its signaling function remains limited. The  
548 emerging studies focusing on H<sub>2</sub>S-mediated persulfidations in plants, especially the recently  
549 reported cases showing the key function of persulfidation in ABA-regulated stomatal  
550 movements, have greatly contributed to the understanding of the H<sub>2</sub>S regulatory mechanism in  
551 plants. Although several aspects regarding H<sub>2</sub>S signaling in plants still await to be assessed, we  
552 believe that they will be solved in the near future by the application of advanced techniques,  
553 such as quantitative proteomics, real-time imaging, and structural biology.

554 Intra/inter disulfide formation and S-glutathionylation are known to be the major redox  
555 mechanisms that protect –SH from overoxidation, with GSH being the most important low  
556 molecular weight antioxidant in the cells. Recently, the reaction rate of SOH with H<sub>2</sub>S has been  
557 reported to be 2700 M<sup>-1</sup>s<sup>-1</sup> (Cuevasanta et al., 2015), which is much faster than that of –SH  
558 (21.6 M<sup>-1</sup>s<sup>-1</sup>) or that of GSH (2.9 M<sup>-1</sup>s<sup>-1</sup>) for the formation of disulfides and -SSG, **respectively**  
559 (Turell et al., 2008). In addition, increased persulfidation has been observed as a response to  
560 H<sub>2</sub>O<sub>2</sub> stress in mammalian cells (Wedmann et al., 2016), indicating that the persulfidation  
561 chemistry involves the preferential addition of H<sub>2</sub>S to a –SOH protein. Furthermore, H<sub>2</sub>S might  
562 play an important role as an antioxidant through persulfidation in protecting thiols from  
563 irreversible overoxidations, such as –SO<sub>3</sub>H. To compare the antioxidant role of H<sub>2</sub>S-mediated

564 persulfidation with that of others PTMs, such as GSH-mediated S-glutathionylation, several  
565 features need to be taken into account, including the cellular concentration of H<sub>2</sub>S in the  
566 microenvironment. The concentrations of H<sub>2</sub>O<sub>2</sub> and GSH in plant cells have been well  
567 documented (Cheeseman, 2006; Hasanuzzaman et al., 2017; Smirnov and Arnaud, 2019) and  
568 measurements at a spatiotemporal resolution of H<sub>2</sub>O<sub>2</sub> and GSH have been improved by means  
569 of genetically encoded sensors (Niemeyer et al., 2021; Nietzel et al., 2019; Ugalde et al., 2021a,  
570 2021b, 2022). Unfortunately, the information on the cellular H<sub>2</sub>S content is scarce. Although  
571 the available H<sub>2</sub>S fluorescent probes provide useful tools to detect H<sub>2</sub>S production *in situ*, the  
572 noninvasive application of chemical fluorescent probes *in planta* for real-time H<sub>2</sub>S  
573 measurements remains a challenge because plant tissues are rather rigid. In our opinion, the  
574 implementation of genetic sensors for spatiotemporal monitoring of H<sub>2</sub>S levels in cells would  
575 greatly advance our understanding of H<sub>2</sub>S signaling in plants.

576 Besides GSH, ascorbate, another abundant antioxidant in plant cells, occurs in all subcellular  
577 compartments with particularly high levels in the chloroplasts (Smirnov and Wheeler, 2000).  
578 Ascorbate-GSH cycle has been recognized as one of the major redox regulation pathways to  
579 detoxify H<sub>2</sub>O<sub>2</sub> in plant cell (Foyer and Noctor, 2011). Although ascorbate was thought to  
580 selectively reduce –SNO formation and had been used extensively for the –SNO protein  
581 identification in proteomic studies (Willems et al., 2021), it has been found to also reduce –  
582 SOH of several proteins, including 1-Cys Prx (Monteiro et al., 2007) and the thiol-specific  
583 antioxidant enzyme 2 (Anschau et al., 2020) from *Saccharomyces cerevisiae* and papain from  
584 *Mus musculus* (Zito et al., 2012). Therefore, concern about the selectivity of ascorbate toward  
585 –SNO in terms of proteomic analysis is increasing. More importantly, these findings hint at an  
586 alternative pathway of thiol redox regulation via ascorbate. As H<sub>2</sub>S is known to react with –  
587 SOH to form –SSH, ascorbate might presumably affect persulfidation of certain proteins  
588 indirectly via reduction of –SOH. Nevertheless, the direct correlation between ascorbate and  
589 H<sub>2</sub>S-mediated persulfidation remains elusive. In addition to ascorbate itself, ascorbate  
590 peroxidase (APX), the enzyme catalyzing the conversion of H<sub>2</sub>O<sub>2</sub> into H<sub>2</sub>O in the presence of  
591 ascorbate, undergoes several types of thiol-based PTMs. The enzymatic activity of cytosolic  
592 APX1 in *Arabidopsis* is enhanced by NO-triggered –SNO formation (Begara-Morales et al.,  
593 2014; Yang et al., 2015) or H<sub>2</sub>S-induced –SSH formation (Aroca et al., 2015) at Cys32. Large-  
594 scale proteomic studies revealed that tAPX and sAPX from chloroplast were also sensitive to  
595 thiol modifications (Huang et al., 2019, Wei et al., 2020). However, which are the exact types  
596 of thiol-based PTMs and how they regulate the biological function of chloroplastic APXs still  
597 await to be explored by functional analysis.

598 To better understand the function of H<sub>2</sub>S-mediated persulfidation, it is crucial to find out the  
599 occupancy of –SSH and its correlation with other thiol-based PTMs. Such a correlation was  
600 evidenced by a comparative analysis based on proteomics data between –SSH and –SOH or –  
601 SH events in mammalian studies (Fu et al., 2020a; Zivanovic et al., 2019) and between –SSH,  
602 –SOH, and –SNO in *Arabidopsis* (Aroca et al., 2021b; Zhang et al., 2021; Zhou et al., 2020).  
603 Likewise many thiol-based PTMs, –SSH sites have been mapped at the whole-proteome level  
604 in mammals (Fu et al., 2020a), but remain uncharted territory in plants. Adoption of advanced  
605 proteomic profiling strategies for identification and quantification of the complete repertoire of  
606 **persulfidation-undergoing** Cys sites in plants will prove a promising future endeavor.

607

#### 608 **Authors' Contributions**

609 J.H. conceived and wrote the article, Y.X. revised and submitted the manuscript.

610

#### 611 **Author Disclosure Statement**

612 No competing financial interests exist.

613

#### 614 **Funding Information**

615 **This work was supported by the Jiangsu Natural Science Foundation for Distinguished Young**  
616 **Scholars [no. BK20220084 to Y.X.], the Fundamental Research Funds for the Central**  
617 **Universities [no. XUEKEN2022002 to Y.X.], and the Research Foundation-Flanders FWO**  
618 **Senior Postdoctoral fellowship [no. 1227020N to J.H.].**

619

#### 620 **Acknowledgment**

621 The authors thank Martine De Cock for her kind support on the manuscript preparation.

622

623 **References**

624

625 Akter S, Fu L, Jung Y, et al. Chemical proteomics reveals new targets of cysteine sulfinic acid  
626 reductase. *Nat Chem Biol* 2018;14(11):995-1004; doi: 10.1038/s41589-018-0116-2.

627 Allison WS. Formation and reactions of sulfenic acids in proteins. *Accounts Chem Res*  
628 1976;9(8):293-299; doi: 10.1021/AR50104A003.

629 Álvarez C, Calo L, Romero LC, et al. An *O*-acetylserine(thiol)lyase homolog with L-cysteine  
630 desulfhydrase activity regulates cysteine homeostasis in *Arabidopsis*. *Plant Physiol*  
631 2010;152(2):656-669; doi: 10.1104/pp.109.147975.

632 Alves R, Vilaprinyo E, Sorribas A, et al. Evolution based on domain combinations: the case of  
633 glutaredoxins. *BMC Evol Biol* 2009;9(1):66; doi: 10.1186/1471-2148-9-66.

634 Anschau V, Ferrer-Sueta G, Aleixo-Silva RL, et al. Reduction of sulfenic acids by ascorbate in  
635 proteins, connecting thiol-dependent to alternative redox pathways. *Free Radic Biol Med*  
636 2020;156:207-216; doi: 10.1016/j.freeradbiomed.2020.06.015.

637 Antoniou C, Xenofontos R, Chatzimichail G, et al. Exploring the potential of nitric oxide and  
638 hydrogen sulfide (NOSH)-releasing synthetic compounds as novel priming agents against  
639 drought stress in *Medicago sativa* plants. *Biomolecules* 2020;10(1):120; doi:  
640 10.3390/biom10010120.

641 Aroca A, Benito JM, Gotor C, et al. Persulfidation proteome reveals the regulation of protein  
642 function by hydrogen sulfide in diverse biological processes in *Arabidopsis*. *J Exp Bot*  
643 2017a;68(17):4915-4927; doi: 10.1093/jxb/erx294.

644 Aroca A, Schneider M, Scheibe R, et al. Hydrogen sulfide regulates the cytosolic/nuclear  
645 partitioning of glyceraldehyde-3-phosphate dehydrogenase by enhancing its nuclear  
646 localization. *Plant Cell Physiol* 2017b;58(6):983-992; doi: 10.1093/pcp/pcx056.

647 Aroca Á, Serna A, Gotor C, et al. *S*-sulfhydration: a cysteine posttranslational modification in  
648 plant systems. *Plant Physiol* 2015;168(1):334-342; doi: 10.1104/pp.15.00009.

649 Aroca A, Yruela I, Gotor C, et al. Persulfidation of ATG18a regulates autophagy under ER  
650 stress in *Arabidopsis*. *Proc Natl Acad Sci USA* 2021a;118(20):e2023604118; doi:  
651 10.1073/pnas.2023604118.

652 Aroca A, Zhang J, Xie Y, et al. Hydrogen sulfide signaling in plant adaptations to adverse  
653 conditions: molecular mechanisms. *J Exp Bot* 2021b;72(16):5893-5904; doi:  
654 10.1093/jxb/erab239.

655 Bagarinao T, Vetter RD. Oxidative detoxification of sulfide by mitochondria of the California  
656 killifish *Fundulus parvipinnis* and the speckled sanddab *Citharichthys sitgmaeus*. *J Comp*  
657 *Physiol B - Biochem Mol Biol* 1990;160(5):519-527; doi: 10.1007/BF00258979.

658 Balsera M, Buchanan BB. Evolution of the thioredoxin system as a step enabling adaptation to  
659 oxidative stress. *Free Radic Biol Med* 2019;140:28-35; doi:  
660 10.1016/j.freeradbiomed.2019.03.003.

661 Baudouin E, Poilevey A, Indiketi Hewage N, et al. The significance of hydrogen sulfide for  
662 Arabidopsis seed germination. *Front Plant Sci* 2016;7:930; doi: 10.3389/fpls.2016.00930.

663 Begara-Morales JC, Sánchez-Calvo B, Chaki M, et al. Dual regulation of cytosolic ascorbate  
664 peroxidase (APX) by tyrosine nitration and S-nitrosylation. *J Exp Bot* 2014;65(2):527-538;  
665 doi: 10.1093/jxb/ert396.

666 Biteau B, Labarre J, Toledano MB. ATP-dependent reduction of cysteine-sulphinic acid by *S.*  
667 *cerevisiae* sulphiredoxin. *Nature* 2003;425(6961):980-984; doi: 10.1038/nature02075.

668 Bloem E, Riemenschneider A, Volker J, et al. Sulphur supply and infection with *Pyrenopeziza*  
669 *brassicae* influence L-cysteine desulphydrase activity in *Brassica napus* L. *J Exp Bot*  
670 2004;55(406):2305-2312; doi: 10.1093/jxb/erh236.

671 Brown EM, Ranasinghe Arachchige NPR, Paudel A, et al. Synthesis, stability, and kinetics of  
672 hydrogen sulfide release of dithiophosphates. *J Agric Food Chem* 2021;69(43):12900-  
673 12908; doi: 10.1021/acs.jafc.1c04655.

674 Burandt P, Papenbrock J, Schmidt A, et al. Genotypical differences in total sulfur contents and  
675 cysteine desulphydrase activities in *Brassica napus* L. *Phyton* 2001;41:75-86.

676 Cannio R, Fiorentino G, Morana A, et al. Oxygen: friend or foe? Archaeal superoxide  
677 dismutases in the protection of intra- and extracellular oxidative stress. *Front Biosci*  
678 2000;5:D768-D779; doi: 10.2741/cannio.

679 Carter JM, Brown EM, Grace JP, et al. Improved growth of pea, lettuce, and radish plants using  
680 the slow release of hydrogen sulfide from GYY-4137. *PLoS ONE* 2018;13(12):e0208732;  
681 doi: 10.1371/journal.pone.0208732.

682 Carter JM, Brown EM, Irish EE, et al. Characterization of dialkyldithiophosphates as slow  
683 hydrogen sulfide releasing chemicals and their effect on the growth of maize. *J Agric Food*  
684 *Chem* 2019;67(43):11883-11892; doi: 10.1021/acs.jafc.9b04398.

685 Cheeseman JM. Hydrogen peroxide concentrations in leaves under natural conditions. *J Exp*  
686 *Bot* 2006;57(10):2435-2444; doi: 10.1093/jxb/erl004.

687 Chen B, Li W, Lv C, et al. Fluorescent probe for highly selective and sensitive detection of  
688 hydrogen sulfide in living cells and cardiac tissues. *Analyst* 2013a;138(3):946-951; doi:  
689 10.1039/c2an36113b.

690 Chen G, Battaglia E, Senay C, et al. Photoaffinity labeling probe for the substrate binding site  
691 of human phenol sulfotransferase (SULT1A1): 7-azido-4-methylcoumarin. *Protein Sci*  
692 1999;8(10):2151-2157; doi: 10.1110/ps.8.10.2151.

693 Chen J, Wu F-H, Wang W-H, et al. Hydrogen sulphide enhances photosynthesis through  
694 promoting chloroplast biogenesis, photosynthetic enzyme expression, and thiol redox  
695 modification in *Spinacia oleracea* seedlings. *J Exp Bot* 2011;62(13):4481-4493; doi:  
696 10.1093/jxb/err145.

697 Chen S, Chen Z-J, Ren W, et al. Reaction-based genetically encoded fluorescent hydrogen  
698 sulfide sensors. *J Am Chem Soc* 2012;134(23):9589-9592; doi: 10.1021/ja303261d.

699 Chen S, Jia H, Wang X, et al. Hydrogen sulfide positively regulates abscisic acid signaling  
700 through persulfidation of SnRK2.6 in guard cells. *Mol Plant* 2020;13(5):732-744; doi:  
701 10.1016/j.molp.2020.01.004.

702 Chen S, Wang X, Jia H, et al. Persulfidation-induced structural change in SnRK2.6 establishes  
703 intramolecular interaction between phosphorylation and persulfidation. *Mol Plant*  
704 2021;14(11):1814-1830; doi: 10.1016/j.molp.2021.07.002.

705 Chen W, Liu C, Peng B, et al. New fluorescent probes for sulfane sulfurs and the application in  
706 bioimaging. *Chem Sci* 2013b;4(7):2892-2896; doi: 10.1039/c3sc50754h.

707 Chen Y, Mo H-Z, Zheng M-Y, et al. Selenium inhibits root elongation by repressing the  
708 generation of endogenous hydrogen sulfide in *Brassica rapa*. *PLoS ONE*  
709 2014;9(10):e110904; doi: 10.1371/journal.pone.0110904.

710 Christou A, Manganaris GA, Papadopoulos I, et al. Hydrogen sulfide induces systemic  
711 tolerance to salinity and non-ionic osmotic stress in strawberry plants through modification  
712 of reactive species biosynthesis and transcriptional regulation of multiple defence pathways.  
713 *J Exp Bot* 2013;64(7):1953-1966; doi: 10.1093/jxb/ert055.

714 Corpas FJ. Hydrogen sulfide: a new warrior against abiotic stress. *Trends Plant Sci*  
715 2019;24(11):983-988; doi: 10.1016/j.tplants.2019.08.003.

716 Corpas FJ, Palma JM. H<sub>2</sub>S signaling in plants and applications in agriculture. *J Adv Res*  
717 2020;24:131-137; doi: 10.1016/j.jare.2020.03.011.

718 Cortese-Krott MM, Koning A, Kuhnle GGC, et al. The reactive species interactome:  
719 evolutionary emergence, biological significance, and opportunities for redox metabolomics

720 and personalized medicine. *Antioxid Redox Signal* 2017;27(10):684-712; doi:  
721 10.1089/ars.2017.7083.

722 Cremlyn RJW. *An Introduction to Organosulfur Chemistry*. Wiley: Chichester, New York;  
723 1996.

724 Cuevasanta E, Lange M, Bonanata J, et al. Reaction of hydrogen sulfide with disulfide and  
725 sulfenic acid to form the strongly nucleophilic persulfide. *J Biol Chem* 2015;290(45):26866-  
726 26880; doi: 10.1074/jbc.M115.672816.

727 Cuevasanta E, Möller MN, Alvarez B. Biological chemistry of hydrogen sulfide and  
728 persulfides. *Arch Biochem Biophys* 2017;617:9-25; doi: 10.1016/j.abb.2016.09.018.

729 Demoulin CF, Lara YJ, Cornet L, et al. Cyanobacteria evolution: insight from the fossil record.  
730 *Free Radic Biol Med* 2019;140:206-223; doi: 10.1016/j.freeradbiomed.2019.05.007.

731 Deng G, Zhou L, Wang Y, et al. Hydrogen sulfide acts downstream of jasmonic acid to inhibit  
732 stomatal development in Arabidopsis. *Planta* 2020;251(2):42; doi: 10.1007/s00425-019-  
733 03334-9.

734 Dietz K-J. Peroxiredoxins in plants and cyanobacteria. *Antioxid Redox Signal*  
735 2011;15(4):1129-1159; doi: 10.1089/ars.2010.3657.

736 Dilek N, Papapetropoulos A, Toliver-Kinsky T, et al. Hydrogen sulfide: an endogenous  
737 regulator of the immune system. *Pharmacol Res* 2020;161:105119; doi:  
738 10.1016/j.phrs.2020.105119.

739 Doeller JE, Gaschen BK, Parrino V, et al. Chemolithoheterotrophy in a metazoan tissue: sulfide  
740 supports cellular work in ciliated mussel gills. *J Exp Biol* 1999;202(14):1953-1961; doi:  
741 10.1242/jeb.202.14.1953.

742 Doeller JE, Grieshaber MK, Kraus DW. Chemolithoheterotrophy in a metazoan tissue:  
743 thiosulfate production matches ATP demand in ciliated mussel gills. *J Exp Biol*  
744 2001;204(21):3755-3764; doi: 10.1242/jeb.204.21.3755.

745 Doeller JE, Isbell TS, Benavides G, et al. Polarographic measurement of hydrogen sulfide  
746 production and consumption by mammalian tissues. *Anal Biochem* 2005;341(1):40-51; doi:  
747 10.1016/j.ab.2005.03.024.

748 Dóka É, Arnér ESJ, Schmidt EE, et al. ProPerDP: a protein persulfide detection protocol.  
749 *Methods Mol Biol* 2019;2007:51-77; doi: 10.1007/978-1-4939-9528-8\_5.

750 Dóka É, Ida T, Dagnell M, et al. Control of protein function through oxidation and reduction of  
751 persulfidated states. *Sci Adv* 2020;6(1):eaax8358; doi: 10.1126/sciadv.aax8358.

752 Dóka É, Pader I, Bíró A, et al. A novel persulfide detection method reveals protein persulfide-  
753 and polysulfide-reducing functions of thioredoxin and glutathione systems. *Sci Adv*  
754 2016;2(1):e1500968; doi: 10.1126/sciadv.1500968.

755 Du X, Jin Z, Liu Z, et al. H<sub>2</sub>S persulfidated and increased kinase activity of MPK4 TO  
756 RESPONSE COLD STress in *Arabidopsis*. *Front Mol Biosci* 2021;8:635470; doi:  
757 10.3389/fmolb.2021.635470.

758 Du X, Jin Z, Zhang L, et al. H<sub>2</sub>S is involved in ABA-mediated stomatal movement through  
759 MPK4 to alleviate drought stress in *Arabidopsis thaliana*. *Plant Soil* 2019;435(1):295-307;  
760 doi: 10.1007/s11104-018-3894-0.

761 Ellis AJ, Golding RM. Spectrophotometric determination of the acid dissociation constants of  
762 hydrogen sulphide. *J. Chem Soc (Resumed)* 1959:127-130; doi: 10.1039/JR9590000127.

763 Feng C-Z, Chen Y, Wang C, et al. *Arabidopsis* RAV1 transcription factor, phosphorylated by  
764 SnRK2 kinases, regulates the expression of *ABI3*, *ABI4*, and *ABI5* during seed germination  
765 and early seedling development. *Plant J* 2014;80(4):654-668; doi: 10.1111/tpj.12670.

766 Filipovic MR. Persulfidation (S-sulphydration) and H<sub>2</sub>S. In: *Chemistry, Biochemistry and*  
767 *Pharmacology of Hydrogen Sulfide*. (Moore PK, Whiteman M eds.) Springer International  
768 Publishing: Cham, 2015; pp. 29-59.

769 Filipovic MR, Zivanovic J, Alvarez B, et al. Chemical biology of H<sub>2</sub>S signaling through  
770 persulfidation. *Chem Rev* 2018;118(3):1253-1337; doi: 10.1021/acs.chemrev.7b00205.

771 Fournier GP, Moore KR, Rangel LT, et al. The Archean origin of oxygenic photosynthesis and  
772 extant cyanobacterial lineages. *Proc R Soc B* 2021;288(1959):20210675; doi:  
773 10.1098/rspb.2021.0675.

774 Fox BC, Slade L, Torregrossa R, et al. The mitochondria-targeted hydrogen sulfide donor AP39  
775 improves health and mitochondrial function in a *C. elegans* primary mitochondrial disease  
776 model. *J Inherit Metab Dis* 2021;44(2):367-375; doi: 10.1002/jimd.12345.

777 Foyer CH, Noctor G. Ascorbate and glutathione: the heart of the redox hub. *Plant Physiol*  
778 2011;155(1):2-18; doi: 10.1104/pp.110.167569.

779 Francoleon NE, Carrington SJ, Fukuto JM. The reaction of H<sub>2</sub>S with oxidized thiols: generation  
780 of persulfides and implications to H<sub>2</sub>S biology. *Arch Biochem Biophys* 2011;516(2):146-  
781 153; doi: 10.1016/j.abb.2011.09.015.

782 Fu L, Liu K, He J, et al. Direct proteomic mapping of cysteine persulfidation. *Antioxid Redox*  
783 *Signal* 2020a;33(15):1061-1076; doi: 10.1089/ars.2019.7777.

784 Fu M-M, Dawood M, Wang N-H, et al. Exogenous hydrogen sulfide reduces cadmium uptake  
785 and alleviates cadmium toxicity in barley. *Plant Growth Regul* 2019;89(2):227-237; doi:  
786 10.1007/s10725-019-00529-8.

787 Fu Y-J, Shen S-S, Guo X-F, et al. A new strategy to improve the water solubility of an organic  
788 fluorescent probe using silicon nanodots and fabricate two-photon SiND-ANPA-N<sub>3</sub> for  
789 visualizing hydrogen sulfide in living cells and onion tissues. *Journal of Materials Chemistry*  
790 *B* 2020b;8(7):1422-1431; doi: 10.1039/c9tb02237f.

791 Fukudome M, Shimada H, Uchi N, et al. Reactive sulfur species interact with other signal  
792 molecules in root nodule symbiosis in *Lotus japonicus*. *Antioxidants* 2020;9(2):145; doi:  
793 10.3390/antiox9020145.

794 Gao X-H, Krokowski D, Guan B-J, et al. Quantitative H<sub>2</sub>S-mediated protein sulfhydration  
795 reveals metabolic reprogramming during the integrated stress response. *eLife*  
796 2015;4:e10067; doi: 10.7554/eLife.10067.

797 Gao X-H, Li L, Parisien M, et al. Discovery of a redox thiol switch: implications for cellular  
798 energy metabolism. *Mol Cell Proteomics* 2020;19(5):852-870; doi:  
799 10.1074/mcp.RA119.001910.

800 **García-Mata C, Lamattina L. Hydrogen sulphide, a novel gasotransmitter involved in guard cell**  
801 **signalling. *New Phytol* 2010;188(4):977-984; doi: 10.1111/j.1469-8137.2010.03465.x.**

802 Ge Y, Hu K-D, Wang S-S, et al. Hydrogen sulfide alleviates postharvest ripening and  
803 senescence of banana by antagonizing the effect of ethylene. *PLoS ONE*  
804 2017;12(6):e0180113; doi: 10.1371/journal.pone.0180113.

805 **Gubern M, Andriamihaja M, Nübel T, et al. Sulfide, the first inorganic substrate for human**  
806 **cells. *FASEB J* 2007;21(8):1699-1706; doi: 10.1096/fj.06-7407com.**

807 Hannestad U, Margheri S, Sörbo B. A sensitive gas chromatographic method for determination  
808 of protein-associated sulfur. *Anal Biochem* 1989;178(2):394-398; doi: 10.1016/0003-  
809 2697(89)90659-3.

810 Harrington HM, Smith IK. Cysteine metabolism in cultured tobacco cells. *Plant Physiol*  
811 1980;65(1):151-155; doi: 10.1104/pp.65.1.151.

812 Hasanuzzaman M, Nahar K, Anee TI, et al. Glutathione in plants: biosynthesis and  
813 physiological role in environmental stress tolerance. *Physiol Mol Biol Plants*  
814 2017;23(2):249-268; doi: 10.1007/s12298-017-0422-2.

815 Hatzfeld Y, Maruyama A, Schmidt A, et al.  $\beta$ -Cyanoalanine synthase is a mitochondrial  
816 cysteine synthase-like protein in spinach and Arabidopsis. *Plant Physiol* 2000;123(3):1163-  
817 1171; doi: 10.1104/pp.123.3.1163.

818 He J, Zhang R-X, Kim DS, et al. ROS of distinct sources and salicylic acid separate elevated  
819 CO<sub>2</sub>-mediated stomatal movements in *Arabidopsis*. *Front Plant Sci* 2020;11:542; doi:  
820 10.3389/fpls.2020.00542.

821 Hess DT, Matsumoto A, Kim S-O, et al. Protein S-nitrosylation: purview and parameters. *Nat*  
822 *Rev Mol Cell Biol* 2005;6(2):150-166; doi: 10.1038/nrm1569.

823 Honda K, Yamada N, Yoshida R, et al. 8-Mercapto-cyclic GMP mediates hydrogen sulfide-  
824 induced stomatal closure in *Arabidopsis*. *Plant Cell Physiol* 2015;56(8):1481-1489; doi:  
825 10.1093/pcp/pcv069.

826 Hou L, Zhu D, Ma Q, et al. H<sub>2</sub>S synthetase *AtD-CDes* involves in ethylene and drought  
827 regulated stomatal movement. *Sci Bull* 2016;61(15):1171-1175; doi: 10.1007/s11434-016-  
828 1128-5.

829 Hu L-Y, Hu S-L, Wu J, et al. Hydrogen sulfide prolongs postharvest shelf life of strawberry  
830 and plays an antioxidative role in fruits. *J Agric Food Chem* 2012;60(35):8684-8693; doi:  
831 10.1021/jf300728h.

832 Huang J, Willems P, Van Breusegem F, et al. Pathways crossing mammalian and plant  
833 sulfenomic landscapes. *Free Radic Biol Med* 2018;122:193-201; doi:  
834 10.1016/j.freeradbiomed.2018.02.012.

835 Huang J, Willems P, Wei B, et al. Mining for protein S-sulfenylation in *Arabidopsis* uncovers  
836 redox-sensitive sites. *Proc Natl Acad Sci USA* 2019;116(42):21256-21261; doi:  
837 10.1073/pnas.1906768116.

838 Hughes MN, Centelles MN, Moore KP. Making and working with hydrogen sulfide: The  
839 chemistry and generation of hydrogen sulfide in vitro and its measurement in vivo: a review.  
840 *Free Radic Biol Med* 2009;47(10):1346-1353; doi: 10.1016/j.freeradbiomed.2009.09.018.

841 Iciek M, Kowalczyk-Pachel D, Bilaska-Wilkosz A, et al. S-sulfhydration as a cellular redox  
842 regulation. *Bioscience Reports* 2015;36(2):e00304; doi: 10.1042/bsr20150147.

843 Jia H, Chen S, Liu D, et al. Ethylene-induced hydrogen sulfide negatively regulates ethylene  
844 biosynthesis by persulfidation of ACO in tomato under osmotic stress. *Front Plant Sci*  
845 2018;9:1517; doi: 10.3389/fpls.2018.01517.

846 Jiang G, Li M, Wen Y, et al. Visualization of sulfane sulfur in plants with a near-infrared  
847 fluorescent probe. *ACS Sensors* 2019;4(2):434-440; doi: 10.1021/acssensors.8b01423.

848 Jin Z, Shen J, Qiao Z, et al. Hydrogen sulfide improves drought resistance in *Arabidopsis*  
849 *thaliana*. *Biochem Biophys Res Commun* 2011;414(3):481-486; doi:  
850 10.1016/j.bbrc.2011.09.090.

851 Jin Z, Wang Z, Ma Q, et al. Hydrogen sulfide mediates ion fluxes inducing stomatal closure in  
852 response to drought stress in *Arabidopsis thaliana*. *Plant Soil* 2017;419(1):141-152; doi:  
853 10.1007/s11104-017-3335-5.

854 Jin Z, Xue S, Luo Y, et al. Hydrogen sulfide interacting with abscisic acid in stomatal regulation  
855 responses to drought stress in *Arabidopsis*. *Plant Physiol Biochem* 2013;62:41-46; doi:  
856 10.1016/j.plaphy.2012.10.017.

857 Ju Y, Wu L, Yang G. Thioredoxin 1 regulation of protein S-desulfhydration. *Biochemistry and*  
858 *Biophysics Reports* 2016;5:27-34; doi: 10.1016/j.bbrep.2015.11.012.

859 Jurado-Flores A, Romero LC, Gotor C. Label-free quantitative proteomic analysis of nitrogen  
860 starvation in *Arabidopsis* root reveals new aspects of H<sub>2</sub>S signaling by protein persulfidation.  
861 *Antioxidants* 2021;10(4):508; doi: 10.3390/antiox10040508.

862 Kabil O, Banerjee R. Redox biochemistry of hydrogen sulfide. *J Biol Chem*  
863 2010;285(29):21903-21907; doi: 10.1074/jbc.R110.128363.

864 Kim TH, Böhmer M, Hu H, et al. Guard cell signal transduction network: advances in  
865 understanding abscisic acid, CO<sub>2</sub>, and Ca<sup>2+</sup> signaling. *Annu Rev Plant Biol* 2010;61:561-  
866 591; doi: 10.1146/annurev-arplant-042809-112226.

867 Kimura H, Shibuya N, Kimura Y. Hydrogen sulfide is a signaling molecule and a  
868 cytoprotectant. *Antioxid Redox Signal* 2012;17(1):45-57; doi: 10.1089/ars.2011.4345.

869 Knoops B, Loumaye E, Van Der Eecken V. Evolution of the peroxiredoxins. *Subcell Biochem*  
870 2007;44:27-40; doi: 10.1007/978-1-4020-6051-9\_2.

871 Kodela R, Chattopadhyay M, Kashfi K. NOSH-aspirin: a novel nitric oxide–hydrogen sulfide-  
872 releasing hybrid: a new class of anti-inflammatory pharmaceuticals. *ACS Med Chem Lett*  
873 2012;3(3):257-262; doi: 10.1021/ml300002m.

874 Kong L, Lu W, Cao X, et al. The design strategies and biological applications of probes for the  
875 gaseous signaling molecule hydrogen sulfide. *Journal of Materials Chemistry B*  
876 2022;10(39):7924-7954; doi: 10.1039/d2tb01210c.

877 Kopriva S, Calderwood A, Weckopp SC, et al. Plant sulfur and Big Data. *Plant Sci* 2015;241:1-  
878 10; doi: 10.1016/j.plantsci.2015.09.014.

879 Kouroussis E, Adhikari B, Zivanovic J, et al. Measurement of protein persulfidation: improved  
880 tag-switch method. *Methods Mol Biol* 2019;2007:37-50; doi: 10.1007/978-1-4939-9528-  
881 8\_4.

882 Laureano-Marín AM, Aroca Á, Pérez-Pérez ME, et al. Abscisic acid-triggered persulfidation  
883 of the Cys protease ATG4 mediates regulation of autophagy by sulfide. *Plant Cell*  
884 2020;32(12):3902-3920; doi: 10.1105/tpc.20.00766.

885 Laureano-Marín AM, García I, Romero LC, et al. Assessing the transcriptional regulation of L-  
886 cysteine desulfhydrase 1 in *Arabidopsis thaliana*. *Front Plant Sci* 2014;5:683; doi:  
887 10.3389/fpls.2014.00683.

888 Le Trionnaire S, Perry A, Szczesny B, et al. The synthesis and functional evaluation of a  
889 mitochondria-targeted hydrogen sulfide donor, (10-oxo-10-(4-(3-thioxo-3H-1,2-dithiol-5-  
890 yl)phenoxy)decyl)triphenylphosphonium bromide (AP39). *MedChemComm*  
891 2014;5(6):728-736; doi: 10.1039/C3MD00323J.

892 Li G, Polk BJ, Meazell LA, et al. ISE analysis of hydrogen sulfide in cigarette smoke. *Journal*  
893 *of Chemical Education* 2000;77(8):1049-1052; doi: 10.1021/ed077p1049.

894 Li J, Chen S, Wang X, et al. Hydrogen sulfide disturbs actin polymerization via S-sulfhydration  
895 resulting in stunted root hair growth. *Plant Physiol* 2018;178(2):936-949; doi:  
896 10.1104/pp.18.00838.

897 Li J, Jia H, Wang J, et al. Hydrogen sulfide is involved in maintaining ion homeostasis via  
898 regulating plasma membrane Na<sup>+</sup>/H<sup>+</sup> antiporter system in the hydrogen peroxide-dependent  
899 manner in salt-stress *Arabidopsis thaliana* root. *Protoplasma* 2014a;251(4):899-912; doi:  
900 10.1007/s00709-013-0592-x.

901 Li L, Whiteman M, Guan YY, et al. Characterization of a novel, water-soluble hydrogen  
902 sulfide-releasing molecule (GYY4137). *Circulation* 2008;117(18):2351-2360; doi:  
903 10.1161/CIRCULATIONAHA.107.753467.

904 Li S-P, Hu K-D, Hu L-Y, et al. Hydrogen sulfide alleviates postharvest senescence of broccoli  
905 by modulating antioxidant defense and senescence-related gene expression. *J Agric Food*  
906 *Chem* 2014b;62(5):1119-1129; doi: 10.1021/jf4047122.

907 Li Y-J, Chen J, Xian M, et al. In site bioimaging of hydrogen sulfide uncovers its pivotal role  
908 in regulating nitric oxide-induced lateral root formation. *PLoS ONE* 2014c;9(2):e90340; doi:  
909 10.1371/journal.pone.0090340.

910 Li Z-G, Gong M, Xie H, et al. Hydrogen sulfide donor sodium hydrosulfide-induced heat  
911 tolerance in tobacco (*Nicotiana tabacum* L) suspension cultured cells and involvement of  
912 Ca<sup>2+</sup> and calmodulin. *Plant Sci* 2012;185-186:185-189; doi: 10.1016/j.plantsci.2011.10.006.

913 Lin VS, Chen W, Xian M, et al. Chemical probes for molecular imaging and detection of  
914 hydrogen sulfide and reactive sulfur species in biological systems. *Chem Soc Rev*  
915 2015;44(14):4596-4618; doi: 10.1039/c4cs00298a.

916 Lisjak M, Srivastava N, Teklic T, et al. A novel hydrogen sulfide donor causes stomatal opening  
917 and reduces nitric oxide accumulation. *Plant Physiol Biochem* 2010;48(12):931-935; doi:  
918 10.1016/j.plaphy.2010.09.016.

919 Lisjak M, Teklić T, Wilson ID, et al. Hydrogen sulfide effects on stomatal apertures. *Plant*  
920 *Signal Behav* 2011;6(10):1444-1446; doi: 10.4161/psb.6.10.17104.

921 Liu C, Pan J, Li S, et al. Capture and visualization of hydrogen sulfide by a fluorescent probe.  
922 *Angew Chem Int Ed Engl* 2011a;50(44):10327-10329; doi: 10.1002/anie.201104305.

923 Liu H, Wang J, Liu J, et al. Hydrogen sulfide (H<sub>2</sub>S) signaling in plant development and stress  
924 responses. *Abiotech* 2021;2(1):32-63; doi: 10.1007/s42994-021-00035-4.

925 Liu J, Hou L, Liu G, et al. Hydrogen sulfide induced by nitric oxide mediates ethylene-induced  
926 stomatal closure of *Arabidopsis thaliana*. *Chinese Sci Bull* 2011b;56(33):3547-3553; doi:  
927 10.1007/s11434-011-4819-y.

928 Luo Y, Zuo Y, Shi G, et al. Progress on the reaction-based methods for detection of endogenous  
929 hydrogen sulfide. *Anal Bioanal Chem* 2022;414(9):2809-2839; doi: 10.1007/s00216-021-  
930 03777-8.

931 Ma X, Zhang L, Pei Z, et al. Hydrogen sulfide promotes flowering in heading Chinese cabbage  
932 by S-sulfhydration of BraFLCs. *Hortic Res* 2021;8(1):19; doi: 10.1038/s41438-020-00453-  
933 3.

934 Margis R, Dunand C, Teixeira FK, et al. Glutathione peroxidase family – an evolutionary  
935 overview. *FEBS J* 2008;275(15):3959-3970; doi: 10.1111/j.1742-4658.2008.06542.x.

936 Mendoza-Cózatl D, Loza-Tavera H, Hernández-Navarro A, et al. Sulfur assimilation and  
937 glutathione metabolism under cadmium stress in yeast, protists and plants. *FEMS Microbiol*  
938 *Rev* 2005;29(4):653-671; doi: 10.1016/j.femsre.2004.09.004.

939 Meyer B, Ward K, Koshlap K, et al. Second dissociation constant of hydrogen sulfide. *Inorg*  
940 *Chem* 1983;22(16):2345-2346; doi: 10.1021/ic00158a027.

941 Miller A-F. Superoxide dismutases: ancient enzymes and new insights. *FEBS Lett*  
942 2012;586(5):585-595; doi: 10.1016/j.febslet.2011.10.048.

943 Mishanina TV, Libiad M, Banerjee R. Biogenesis of reactive sulfur species for signaling by  
944 hydrogen sulfide oxidation pathways. *Nat Chem Biol* 2015;11(7):457-464; doi:  
945 10.1038/nchembio.1834.

946 Monteiro G, Horta BB, Pimenta DC, et al. Reduction of 1-Cys peroxiredoxins by ascorbate  
947 changes the thiol-specific antioxidant paradigm, revealing another function of vitamin C.  
948 *Proc Natl Acad Sci USA* 2007;104(12):4886-4891; doi: 10.1073/pnas.0700481104.

949 Moseler A, Dhalleine T, Rouhier N, et al. *Arabidopsis thaliana* 3-mercaptopyruvate  
950 sulfurtransferases interact with and are protected by reducing systems. *J Biol Chem*  
951 2021;296:100429; doi: 10.1016/j.jbc.2021.100429.

952 Müller-Schüssele SJ, Schwarzländer M, Meyer AJ. Live monitoring of plant redox and energy  
953 physiology with genetically encoded biosensors. *Plant Physiol* 2021;186(1):93-109; doi:  
954 10.1093/plphys/kiab019.

955 Murphy B, Bhattacharya R, Mukherjee P. Hydrogen sulfide signaling in mitochondria and  
956 disease. *FASEB J* 2019;33(12):13098-13125; doi: 10.1096/fj.201901304R.

957 Mustafa AK, Gadalla MM, Sen N, et al. H<sub>2</sub>S signals through protein S-sulfhydration. *Sci Signal*  
958 2009;2(96):ra72; doi: 10.1126/scisignal.2000464.

959 **Nagy P, Winterbourn CC. Redox chemistry of biological thiols. In: *Advances in Molecular*  
960 *Toxicology*. (Fishbein JC ed.) Elsevier: 2010; pp. 183-222.**

961 Niemeyer J, Scheuring D, Oestreicher J, et al. Real-time monitoring of subcellular H<sub>2</sub>O<sub>2</sub>  
962 distribution in *Chlamydomonas reinhardtii*. *Plant Cell* 2021;33(9):2935-2949; doi:  
963 10.1093/plcell/koab176.

964 Nietzel T, Elsässer M, Ruberti C, et al. The fluorescent protein sensor roGFP2-Orp1 monitors  
965 *in vivo* H<sub>2</sub>O<sub>2</sub> and thiol redox integration and elucidates intracellular H<sub>2</sub>O<sub>2</sub> dynamics during  
966 elicitor-induced oxidative burst in *Arabidopsis*. *New Phytol* 2019;221(3):1649-1664; doi:  
967 10.1111/nph.15550.

968 Olson KR, Straub KD. The role of hydrogen sulfide in evolution and the evolution of hydrogen  
969 sulfide in metabolism and signaling. *Physiology* 2016;31(1):60-72; doi:  
970 10.1152/physiol.00024.2015.

971 Pan J, Carroll KS. Persulfide reactivity in the detection of protein S-sulfhydration. *ACS Chem*  
972 *Biol* 2013;8(6):1110-1116; doi: 10.1021/cb4001052.

973 **Pantaleno R, Scuffi D, Costa A, et al. Mitochondrial H<sub>2</sub>S donor AP39 induces stomatal closure  
974 by modulating guard cell mitochondrial activity. *Plant Physiol* 2023;in press; doi:  
975 10.1093/plphys/kiac591.**

976 **Papanatsiou M, Scuffi D, Blatt MR, et al. Hydrogen sulfide regulates inward-rectifying K<sup>+</sup>  
977 channels in conjunction with stomatal closure. *Plant Physiol* 2015;168(1):29-35; doi:  
978 10.1104/pp.114.256057.**

979 Parent A, Elduque X, Cornu D, et al. Mammalian frataxin directly enhances sulfur transfer of  
980 NFS1 persulfide to both ISCU and free thiols. *Nat Commun* 2015;6:5686; doi:  
981 10.1038/ncomms6686.

982 **Parrino V, Kraus DW, Doeller JE. ATP production from the oxidation of sulfide in gill  
983 mitochondria of the ribbed mussel *Geukensia demissa*. *J Exp Biol* 2000;203(14):2209-2218;  
984 doi: 10.1242/jeb.203.14.2209.**

985 Paulsen CE, Carroll KS. Cysteine-mediated redox signaling: chemistry, biology, and tools for  
986 discovery. *Chem Rev* 2013;113(7):4633-4679; doi: 10.1021/cr300163e.

987 Pilon-Smits EAH, Garifullina GF, Abdel-Ghany S, et al. Characterization of a NifS-like  
988 chloroplast protein from *Arabidopsis*. Implications for its role in sulfur and selenium  
989 metabolism. *Plant Physiol* 2002;130(3):1309-1318; doi: 10.1104/pp.102.010280.

990 Planavsky NJ, Asael D, Hofmann A, et al. Evidence for oxygenic photosynthesis half a billion  
991 years before the Great Oxidation Event. *Nat Geosci* 2014;7(4):283-286; doi:  
992 10.1038/ngeo2122.

993 Pomeroy R. Hydrogen sulfide in sewage. *Sewage Works J* 1941;13(3):498-505.

994 Poole LB, Klomsiri C, Knaggs SA, et al. Fluorescent and affinity-based tools to detect cysteine  
995 sulfenic acid formation in proteins. *Bioconjugate Chem* 2007;18(6):2004-2017; doi:  
996 10.1021/bc700257a.

997 Powell CR, Dillon KM, Matson JB. A review of hydrogen sulfide (H<sub>2</sub>S) donors: Chemistry and  
998 potential therapeutic applications. *Biochem Pharmacol* 2018;149:110-123; doi:  
999 10.1016/j.bcp.2017.11.014.

1000 Räsänen J. Sulfur. In: *Encyclopedia of Analytical Science*. (Worsfold P, Townshend A, Poole  
1001 C eds.) Elsevier: Oxford, 2005; pp. 415-423.

1002 Sakurai H, Ogawa T, Shiga M, et al. Inorganic sulfur oxidizing system in green sulfur bacteria.  
1003 *Photosynth Res* 2010;104(2):163-176; doi: 10.1007/s11120-010-9531-2.

1004 Scuffi D, Álvarez C, Laspina N, et al. Hydrogen sulfide generated by L-cysteine desulfhydrase  
1005 acts upstream of nitric oxide to modulate abscisic acid-dependent stomatal closure. *Plant*  
1006 *Physiol* 2014;166(4):2065-2076; doi: 10.1104/pp.114.245373.

1007 Scuffi D, Nietzel T, Di Fino LM, et al. Hydrogen sulfide increases production of NADPH  
1008 oxidase-dependent hydrogen peroxide and phospholipase D-derived phosphatidic acid in  
1009 guard cell signaling. *Plant Physiol Biochem* 2018;176(3):2532-2542; doi:  
1010 10.1104/pp.17.01636.

1011 Sen N, Paul BD, Gadalla MM, et al. Hydrogen sulfide-linked sulfhydration of NF-κB mediates  
1012 its antiapoptotic actions. *Mol Cell* 2012;45(1):13-24; doi: 10.1016/j.molcel.2011.10.021.

1013 Shatalin K, Shatalina E, Mironov A, et al. H<sub>2</sub>S: a universal defense against antibiotics in  
1014 bacteria. *Science* 2011;334(6058):986-990; doi: 10.1126/science.1209855.

1015 Shen J, Xing T, Yuan H, et al. Hydrogen sulfide improves drought tolerance in *Arabidopsis*  
1016 *thaliana* by microRNA expressions. *PLoS ONE* 2013;8(10):e77047; doi:  
1017 10.1371/journal.pone.0077047.

1018 Shen J, Zhang J, Zhou M, et al. Persulfidation-based modification of cysteine desulfhydrase  
1019 and the NADPH oxidase RBOHD controls guard cell abscisic acid signaling. *Plant Cell*  
1020 2020;32(4):1000-1017; doi: 10.1105/tpc.19.00826.

1021 Shen X, Pattillo CB, Pardue S, et al. Measurement of plasma hydrogen sulfide in vivo and in  
1022 vitro. *Free Radic Biol Med* 2011;50(9):1021-1031; doi:  
1023 10.1016/j.freeradbiomed.2011.01.025.

1024 Siegel LM. A direct microdetermination for sulfide. *Anal Biochem* 1965;11(1):126-132; doi:  
1025 10.1016/0003-2697(65)90051-5.

1026 Smirnov N, Arnaud D. Hydrogen peroxide metabolism and functions in plants. *New Phytol*  
1027 2019;221(3):1197-1214; doi: 10.1111/nph.15488.

1028 Smirnov N, Wheeler GL. Ascorbic acid in plants: biosynthesis and function. *Crit Rev Biochem*  
1029 *Mol Biol* 2000;35(4):291-314; doi: 10.1080/10409230008984166.

1030 Soon F-F, Ng L-M, Zhou XE, et al. Molecular mimicry regulates ABA signaling by SnRK2  
1031 kinases and PP2C phosphatases. *Science* 2012;335(6064):85-88; doi:  
1032 10.1126/science.1215106.

1033 Szczesny B, Módis K, Yanagi K, et al. AP39, a novel mitochondria-targeted hydrogen sulfide  
1034 donor, stimulates cellular bioenergetics, exerts cytoprotective effects and protects against  
1035 the loss of mitochondrial DNA integrity in oxidatively stressed endothelial cells *in vitro*.  
1036 *Nitric Oxide* 2014;41:120-130; doi: 10.1016/j.niox.2014.04.008.

1037 Takahashi H, Buchner P, Yoshimoto N, et al. Evolutionary relationships and functional  
1038 diversity of plant sulfate transporters. *Front Plant Sci* 2012;2:119; doi:  
1039 10.3389/fpls.2011.00119.

1040 Takahashi H, Kopriva S, Giordano M, et al. Sulfur assimilation in photosynthetic organisms:  
1041 molecular functions and regulations of transporters and assimilatory enzymes. *Annu Rev*  
1042 *Plant Biol* 2011;62:157-184; doi: 10.1146/annurev-arplant-042110-103921.

1043 Tang Q, Pang K, Yuan X, et al. A one-billion-year-old multicellular chlorophyte. *Nature Ecol*  
1044 *Evol* 2020;4(4):543-549; doi: 10.1038/s41559-020-1122-9.

1045 Tishel M, Mazelis M. Enzymatic degradation of L-cystine by cytoplasmic particles from  
1046 cabbage leaves. *Nature* 1966;211(5050):745-746; doi: 10.1038/211745a0.

1047 Turell L, Botti H, Carballal S, et al. Reactivity of sulfenic acid in human serum albumin.  
1048 *Biochemistry* 2008;47(1):358-367; doi: 10.1021/bi701520y.

1049 Turell L, Steglich M, Torres MJ, et al. Sulfenic acid in human serum albumin: reaction with  
1050 thiols, oxidation and spontaneous decay. *Free Radic Biol Med* 2021;165:254-264; doi:  
1051 10.1016/j.freeradbiomed.2021.01.039.

1052 Ugalde JM, Fecker L, Schwarzländer M, et al. Live monitoring of ROS-induced cytosolic redox  
1053 changes with roGFP2-based sensors in plants. *Methods Mol Biol* 2022;2526:65-85; doi:  
1054 10.1007/978-1-0716-2469-2\_5.

1055 Ugalde JM, Fuchs P, Nietzel T, et al. Chloroplast-derived photo-oxidative stress causes changes  
1056 in H<sub>2</sub>O<sub>2</sub> and EGSH in other subcellular compartments. *Plant Physiol* 2021a;186(1):125-141;  
1057 doi: 10.1093/plphys/kiab095.

1058 Ugalde JM, Schlößer M, Dongois A, et al. The latest HyPe(r) in plant H<sub>2</sub>O<sub>2</sub> biosensing. *Plant*  
1059 *Physiol Biochem* 2021b;187(2):480-484; doi: 10.1093/plphys/kiab306.

1060 Van Hoewyk D, Pilon M, Pilon-Smits EAH. The functions of NifS-like proteins in plant sulfur  
1061 and selenium metabolism. *Plant Sci* 2008;174(2):117-123; doi:  
1062 10.1016/j.plantsci.2007.10.004.

1063 Vökel S, Grieshaber MK. Sulphide oxidation and oxidative phosphorylation in the  
1064 mitochondria of the lugworm *Arenicola marina*. *J Exp Biol* 1997;200(1):83-92; doi:  
1065 10.1242/jeb.200.1.83.

1066 Wang J, Xie H, Li H, et al. NIR fluorescent probe for *in situ* bioimaging of endogenous H<sub>2</sub>S in  
1067 rice roots under Al<sup>3+</sup> and flooding stresses. *J Agric Food Chem* 2021;69(47):14330-14339;  
1068 doi: 10.1021/acs.jafc.1c05247.

1069 Wang P, Du Y, Hou Y-J, et al. Nitric oxide negatively regulates abscisic acid signaling in guard  
1070 cells by S-nitrosylation of OST1. *Proc Natl Acad Sci USA* 2015;112(2):613-618; doi:  
1071 10.1073/pnas.1423481112.

1072 Wang R. Two's company, three's a crowd: can H<sub>2</sub>S be the third endogenous gaseous  
1073 transmitter? *FASEB J* 2002;16(13):1792-1798; doi: 10.1096/fj.02-0211hyp.

1074 Wang R. Gasotransmitters: growing pains and joys. *Trends Biochem Sci* 2014;39(5):227-232;  
1075 doi: 10.1016/j.tibs.2014.03.003.

1076 Wedmann R, Onderka C, Wei S, et al. Improved tag-switch method reveals that thioredoxin  
1077 acts as depersulfidase and controls the intracellular levels of protein persulfidation. *Chem*  
1078 *Sci* 2016;7(5):3414-3426; doi: 10.1039/c5sc04818d.

1079 Wei B, Willems P, Huang J, et al. Identification of sulfenylated cysteines in *Arabidopsis*  
1080 *thaliana* proteins using a disulfide-linked peptide reporter. *Front Plant Sci* 2020;11:777; doi:  
1081 10.3389/fpls.2020.00777.

1082 Willems P, Van Breusegem F, Huang J. Contemporary proteomic strategies for cysteine  
1083 redoxome profiling. *Plant Physiol* 2021;186(1):110-124; doi: 10.1093/plphys/kiab074.

1084 Wind JJ, Peviani A, Snel B, et al. ABI4: versatile activator and repressor. *Trends Plant Sci*  
1085 2013;18(3):125-132; doi: 10.1016/j.tplants.2012.10.004.

1086 Yamasaki H, Cohen MF. Biological consilience of hydrogen sulfide and nitric oxide in plants:  
1087 gases of primordial earth linking plant, microbial and animal physiologies. *Nitric Oxide*  
1088 2016;55-56:91-100; doi: 10.1016/j.niox.2016.04.002.

1089 Yang H, Mu J, Chen L, et al. S-nitrosylation positively regulates ascorbate peroxidase activity  
1090 during plant stress responses. *Plant Physiol* 2015;167(4):1604-1615; doi:  
1091 10.1104/pp.114.255216.

1092 Yang Z, Wang X, Feng J, et al. Biological functions of hydrogen sulfide in plants. *Int J Mol Sci*  
1093 2022;23(23):15107; doi: 10.3390/ijms232315107.

1094 Yong R, Searcy DG. Sulfide oxidation coupled to ATP synthesis in chicken liver mitochondria.  
1095 *Comp Biochem Physiol B - Biochem Mol Biol* 2001;129(1):129-137; doi: 10.1016/S1096-  
1096 4959(01)00309-8.

1097 Youssef S, Zhang S, Ai H-W. A genetically encoded, ratiometric fluorescent biosensor for  
1098 hydrogen sulfide. *ACS Sensors* 2019;4(6):1626-1632; doi: 10.1021/acssensors.9b00400.

1099 Yun B-W, Feechan A, Yin M, et al. S-nitrosylation of NADPH oxidase regulates cell death in  
1100 plant immunity. *Nature* 2011;478(7368):264-268; doi: 10.1038/nature10427.

1101 Zamocky M, Furtmüller PG, Obinger C. Evolution of catalases from bacteria to humans.  
1102 *Antioxid Redox Signal* 2008;10(9):1527-1548; doi: 10.1089/ars.2008.2046.

1103 Zeng X, Chen W, Liu C, et al. Fluorescence probes for reactive sulfur species in agricultural  
1104 chemistry. *J Agric Food Chem* 2021;69(46):13700-13712; doi: 10.1021/acs.jafc.1c05249.

1105 Zhang D, Macinkovic I, Devarie-Baez NO, et al. Detection of protein S-sulfhydration by a tag-  
1106 switch technique. *Angew Chem Int Ed Engl* 2014;53(2):575-581; doi:  
1107 10.1002/anie.201305876.

1108 Zhang H, Hu S-L, Zhang Z-J, et al. Hydrogen sulfide acts as a regulator of flower senescence  
1109 in plants. *Postharvest Biology and Technology* 2011;60(3):251-257; doi:  
1110 10.1016/j.postharvbio.2011.01.006.

1111 Zhang J, Zhou M, Ge Z, et al. Abscisic acid-triggered guard cell L-cysteine *desulfhydrase*  
1112 function and in situ hydrogen sulfide production contributes to heme oxygenase-modulated  
1113 stomatal closure. *Plant Cell Environ* 2020a;43(3):624-636; doi: 10.1111/pce.13685.

1114 Zhang J, Zhou M, Zhou H, et al. Hydrogen sulfide, a signaling molecule in plant stress  
1115 responses. *J Integr Plant Biol* 2021;63(1):146-160; doi: 10.1111/jipb.13022.

1116 Zhang Q, Cai W, Ji T-T, et al. WRKY13 enhances cadmium tolerance by promoting *D-*  
1117 *CYSTEINE DESULFHYDRASE* and hydrogen sulfide production. *Plant Physiol*  
1118 2020b;183(1):345-357; doi: 10.1104/pp.19.01504.

- 1119 Zhao D, Zhang J, Zhou M, et al. Current approaches for detection of hydrogen sulfide and  
1120 persulfidation in biological systems. *Plant Physiol Biochem* 2020;155:367-373; doi:  
1121 10.1016/j.plaphy.2020.08.006.
- 1122 Zhou H, Zhang J, Shen J, et al. Redox-based protein persulfidation in guard cell ABA signaling.  
1123 *Plant Signal Behav* 2020;15(5):1741987; doi: 10.1080/15592324.2020.1741987.
- 1124 Zhou M, Zhang J, Shen J, et al. Hydrogen sulfide-linked persulfidation of ABI4 controls ABA  
1125 responses through the transactivation of MAPKKK18 in *Arabidopsis*. *Mol Plant*  
1126 2021;14(6):921-936; doi: 10.1016/j.molp.2021.03.007.
- 1127 Zito E, Hansen HG, Yeo GSH, et al. Endoplasmic reticulum thiol oxidase deficiency leads to  
1128 ascorbic acid depletion and noncanonical scurvy in mice. *Mol Cell* 2012;48(1):39-51; doi:  
1129 10.1016/j.molcel.2012.08.010.
- 1130 Zivanovic J, Kouroussis E, Kohl JB, et al. Selective persulfide detection reveals evolutionarily  
1131 conserved antiaging effects of S-sulfhydration. *Cell Metab* 2019;30(6):1152-1170; doi:  
1132 10.1016/j.cmet.2019.10.007.
- 1133 Zou H, Zhang N-N, Pan Q, et al. Hydrogen sulfide promotes nodulation and nitrogen fixation  
1134 in soybean-rhizobia symbiotic system. *Mol Plant-Microbe Interact* 2019;32(8):972-985; doi:  
1135 10.1094/mpmi-01-19-0003-r.

1136 **Figure legends**

1137

1138 **FIG. 1. Sulfur oxidation states in some biologically relevant compounds.** The oxidation  
1139 states of sulfur in different organic and inorganic compounds range from  $-2$  to  $+6$ . R refers to  
1140 the remainder of the molecule and symbolizes the variable side chain in protein structures.

1141

1142 **FIG. 2. H<sub>2</sub>S biosynthesis in plant cells.** H<sub>2</sub>S is produced in different subcellular organelles in  
1143 the plant cells via various enzymes. The assimilated sulfate in plant cells is transported to the  
1144 chloroplasts, where the sulfate is reduced first to APS, then to sulfite that is subsequently  
1145 reduced to sulfide (H<sub>2</sub>S) via SiR. Sulfide can be further catalyzed by OAS-TL in the presence  
1146 of OAS to generate cysteine. In chloroplasts, this reaction is catalyzed by OASB, while the  
1147 same reaction is catalyzed by OASA1 in the cytosol and by OASC in mitochondria. In the  
1148 cytosol, L-cysteine and D-cysteine are degraded by L-CDes and D-CDes, respectively, to  
1149 produce H<sub>2</sub>S, pyruvate, and NH<sub>3</sub>. Thus far, DES1 is the best H<sub>2</sub>S-producing enzyme. NifS has  
1150 been suggested to catalyze cysteine to H<sub>2</sub>S in chloroplasts and mitochondria. In mitochondria,  
1151 CAS catalyzes the reaction of cyanide and L-cysteine to produce H<sub>2</sub>S and  $\beta$ -cyanoalanine.  
1152 Abbreviations: APS, adenosine 5'-phosphosulfate; CAS,  $\beta$ -cyanoalanine synthase; DES1, L-  
1153 cysteine desulfhydrase 1; D-CDes, D-cysteine desulfhydrase; H<sub>2</sub>S, hydrogen sulfide; L-CDe, L-  
1154 cysteine desulfhydrase; NH<sub>3</sub>, ammonia; NifS, nitrogenase Fe-S cluster; OAS, O-acetylserine;  
1155 OAS-TL, O-acetylserine (thiol)lyase; SiR, sulfite reductase.

1156

1157 **FIG. 3. H<sub>2</sub>S detection with fluorescent probes in plants.** Various fluorescent probes have  
1158 been used to visualize and determine the H<sub>2</sub>S level in different plant species. In the chemical  
1159 structures, the red star highlights the reaction moiety for H<sub>2</sub>S and the yellow color marks the  
1160 fluorophore group. AcMZ is a azide (N<sub>3</sub>)-based chemical probe, used to determine the H<sub>2</sub>S level  
1161 in guard cells induced by ABA in wild-type *Arabidopsis* (accession Columbia-0 [Col-0]), but  
1162 not in *des1* mutant plants, whereas the H<sub>2</sub>S donor NaHS induced H<sub>2</sub>S production in the guard  
1163 cells of both genotypes (Zhang et al., 2020a). Another azide-based probe, SiND-ANPA-N<sub>3</sub>, had  
1164 been tested in inner-layer epidermal tissues of onion (Fu et al., 2020b). A nucleophilic reaction-  
1165 based chemical probe, WSP-1, containing a pyridyl disulfide moiety as H<sub>2</sub>S reaction sites, has  
1166 been used in tomato roots to determine H<sub>2</sub>S induction upon nitric oxide donor and scavenger  
1167 treatments, and in the root of turnip for the observation of H<sub>2</sub>S production repression upon  
1168 selenium treatment (Chen et al., 2014). Two sulfane sulfur probes, SSP4 and SSNIP, both  
1169 contain thiophenol moiety. The SSP4 probe has been used to reveal the H<sub>2</sub>S production during

1170 symbiosis in the nodules of *Lotus japonicus* (Fukudome et al., 2020). SSNIP is a recent NIR  
1171 probe used in *Arabidopsis* roots (Jiang et al., 2019). The most recent fluorescent probe applied  
1172 in plants is the NIR-based probe, HBTP-H<sub>2</sub>S, showing an increased H<sub>2</sub>S level upon Al<sup>3+</sup> and  
1173 flooding stresses (Wang et al., 2021). Abbreviations: ABA, abscisic acid; AcMZ, 7-azido-4-  
1174 methylcoumarin; Al<sup>3+</sup>, aluminum ion; BF, bright field; HBTP-H<sub>2</sub>S, 2-(2-hydroxyphenyl)  
1175 benzothiazole--based H<sub>2</sub>S probe; H<sub>2</sub>S, hydrogen sulfide; NIR, near-infrared; SiND-ANPA-N<sub>3</sub>,  
1176 silicon nanodots-4-azido-N-alanine-1,8-naphthalimide; SSP4, sulfane sulfur probe 4; SSNIP,  
1177 sulfane sulfur near-infrared probe; WSP-1, Washington State probe-1.

1178

1179 **FIG. 4. Overview of cysteine thiols undergoing different oxidative posttranslational**  
1180 **modifications.** Protein cysteine –SH reacts with H<sub>2</sub>O<sub>2</sub> to form –SOH that can be further  
1181 oxidized by H<sub>2</sub>O<sub>2</sub> to –SO<sub>2</sub>H and –SO<sub>3</sub>H, both considered protein overoxidations. Via an ATP-  
1182 dependent reaction –SO<sub>2</sub>H can be reduced by SRX, whereas –SO<sub>3</sub>H is an irreversible  
1183 modification. The –SOH protein can react with –SH or with GSH to form –SS– or –SSG,  
1184 respectively. The proteins –SS– and –SSG can be reduced by redoxins, including TRXs and  
1185 GRXs. The protein cysteine –SH reacts with NO to form –SNO that can also be reduced by  
1186 redoxins. H<sub>2</sub>S reacts with –SOH and –SS– to form –SSH, which has been suggested to be  
1187 formed also by the reaction of H<sub>2</sub>S with –SNO or –SSG. The protein –SSH can be oxidized by  
1188 H<sub>2</sub>O<sub>2</sub> to form –SSOH, –SSO<sub>2</sub>H, and –SSO<sub>3</sub>H and –SSH and its oxidative derivatives can be  
1189 reduced by redoxins. Abbreviation: GSH, glutathione; H<sub>2</sub>O<sub>2</sub>, hydrogen peroxide; H<sub>2</sub>S, hydrogen  
1190 peroxide; NO, nitric oxide; –SH, thiol; –SOH; sulfenic acid; –SO<sub>2</sub>H, sulfinic acid; –SO<sub>3</sub>H,  
1191 sulfonic acid; SRX, sulfiredoxin; –SS–, intra/intermolecular disulfides; –SSG, glutathione  
1192 adduct; –SSOH, perthiosulfenic acid; –SSO<sub>2</sub>H, perthiosulfinic acid; –SSO<sub>3</sub>H, perthiosulfonic  
1193 acid; –SNO, S-nitrosothiol.

1194

1195 **FIG. 5. Persulfidation detection approaches. (A) Red maleimide and MalP methods. Both –**  
1196 **SH and –SSH are initially labeled, but only the labeled –SSH can be reduced by DTT. In the**  
1197 **red maleimide method, –SSH is detected by SDS-PAGE and displays fluorescence loss. As the**  
1198 **Mal-P labeling results in an molecular mass increase of 1.95 kDa, –SSH is discovered as a**  
1199 **decreased mobility shift in SDS-PAGE. (B) BTA method for proteomic analysis. Both –SH and**  
1200 **–SSH are labeled with maleimide-biotin and enriched by streptavidin magnetic beads. The**  
1201 **enriched –SSH proteins are eluted by DTT reduction, digested with trypsin, and subjected to**  
1202 **MS analysis. (C) Tag switch and dimedone switch methods. In the tag switch method, MSBT**  
1203 **is used to block both –SH and –SSH, the latter forming –SS–MSBT that further reacts with CN-**

1204 biotin to be biotinylated, which is further enriched by streptavidin AP, digested by trypsin, and  
1205 subjected to MS analysis. Alternatively, CN-BOT and CN-Cy3 are used instead of CN-biotin  
1206 to visualize –SSH *in situ* by confocal microscopy and in-gel fluorescent detection, respectively.  
1207 In the dimedone switch assay, NBF-Cl reacts with –SSH, –SH, and –SOH, whereafter DCP-  
1208 Bio1 or DCP-N3 is added to selectively switch with the –SS–NBF adducts. When DCP-Bio1  
1209 is utilized, the –SSH proteins are subsequently enriched with streptavidin AP and identified by  
1210 MS. When DCP-N<sub>3</sub> and the Cy5-alkyne click mix are applied, the –SSH is detected by in-gel  
1211 fluorescent assay or with confocal microscopy. (D). Direct labeling method at low pH for  
1212 proteomic analysis. Both –SH and –SSH are labeled by IPM at pH 5.0, resulting in proteins  
1213 with S-IPM and SS-IPM adducts that are further digested by trypsin. The digested peptides are  
1214 biotinylated by a click reaction with Az-UV-biotin reagents, enriched by streptavidin AP,  
1215 cleaved by UV light to remove the biotin moiety, and subjected to MS analysis. Abbreviations:  
1216 AP, affinity purification; Az-UV-biotin, UV cleavable biotin-azide; BTA, biotin thiol assay;  
1217 CN-biotin, cyanoacetate biotin; CN-BOT, cyanoacetate with fluorescent BODIPY moiety; CN-  
1218 Cy3, cyanoacetate with Cy3-dye; DCP-Bio1, dimedone-based biotin-conjugated analog; DCP-  
1219 N<sub>3</sub>, dimedone-based azide-conjugated analog; DTT, dithiothreitol; IPM, *N*-  
1220 propynyliodoacetamide; MalP, maleimide-peptide; MSBT, methylsulfonyl benzothiazole;  
1221 NBF-Cl, 4-chloro-7-nitrobenzofurazan; SDS-PAGE, sodium dodecyl sulfate-polyacrylamide  
1222 gel electrophoresis; –SH, thiol; –SSH, persulfide; –SOH, sulfenic acid.

1223

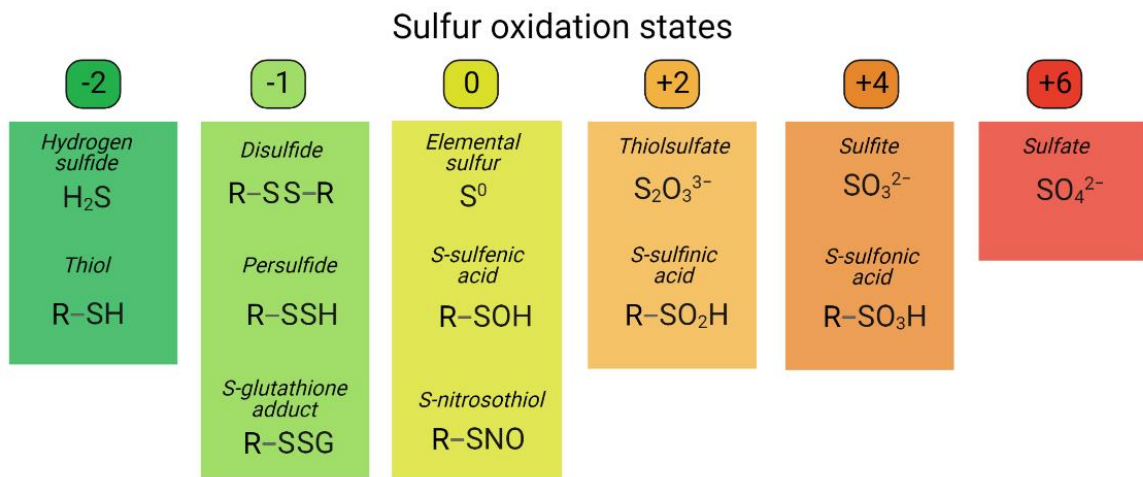
1224 **FIG. 6. Simplified scheme of H<sub>2</sub>S-triggered stomatal closure in ABA-regulated stomatal**  
1225 **closure under drought stress.** Under drought or cold stress, ABA or other phytohormones,  
1226 such as ET, SA, and JA, accumulate in the cells and regulate stomatal movement via H<sub>2</sub>S  
1227 signaling. ABA induces the expression of *DES1*, increasing the H<sub>2</sub>S production. DES1-  
1228 catalyzed H<sub>2</sub>S signals activate downstream H<sub>2</sub>O<sub>2</sub> and NO signaling to trigger stomatal closure.  
1229 Abbreviations: ABA, abscisic acid; DES1, L-cysteine desulhydrase 1; ET, ethylene; H<sub>2</sub>S,  
1230 hydrogen sulfide; H<sub>2</sub>O<sub>2</sub>, hydrogen peroxide; JA, jasmonic acid; NO, nitric oxide; SA, salicylic  
1231 acid.

1232

1233 **FIG. 7. H<sub>2</sub>S-triggered persulfidation in ABA-regulated guard cell movement.** When ABA  
1234 is present, it binds PYR/PYL/RCAR to form a receptor complex that interacts with and inhibits  
1235 the catalytic activity of PP2C, activating SnRK2.6. SnRK2.6 undergoes H<sub>2</sub>S-triggered  
1236 persulfidation, thereby promoting its activity and interaction with ABF2. SnRK2  
1237 phosphorylates downstream the transcription factor RAV1, hampering the expression of

1238 ABI4, whereas DES1-mediated H<sub>2</sub>S production induces ABI4 persulfidation that enhances its  
1239 transactivation activity on *MAPKKK18*, thereby initiating a MAPK cascade. DES1-mediated  
1240 H<sub>2</sub>S triggers its autopersulfidation, leading to a H<sub>2</sub>S burst. The H<sub>2</sub>S accumulation induces  
1241 RBOHD persulfidation, thereby increasing its activity and leading to ROS overproduction. The  
1242 ROS accumulation increases the Ca<sup>2+</sup> influx, contributing to stomata closure in response to  
1243 ABA. Abbreviations: ABA, abscisic acid; ABF2, ABA response element-binding factor 2;  
1244 ABI4, ABA insensitive 4; Ca<sup>2+</sup>, calcium cation; DES1, L-cysteine desulhydrase 1; H<sub>2</sub>S,  
1245 hydrogen sulfide; MAPK, mitogen-activated protein kinase; *MAPKKK18*, *MAPK kinase kinase*  
1246 *18*; PP2C, protein phosphatase type 2C; PYR/PYL/RCAR, PYRABACTIN  
1247 RESISTANCE/PYR-LIKE/REGULATORY COMPONENT OF ABA RECEPTOR; RAV1,  
1248 ABI3/VP1-like 1; RBOHD, respiratory burst oxidase homolog D; SnRK2.6, SNF1-RELATED  
1249 PROTEIN KINASE2.6; ROS, reactive oxygen species.

1250

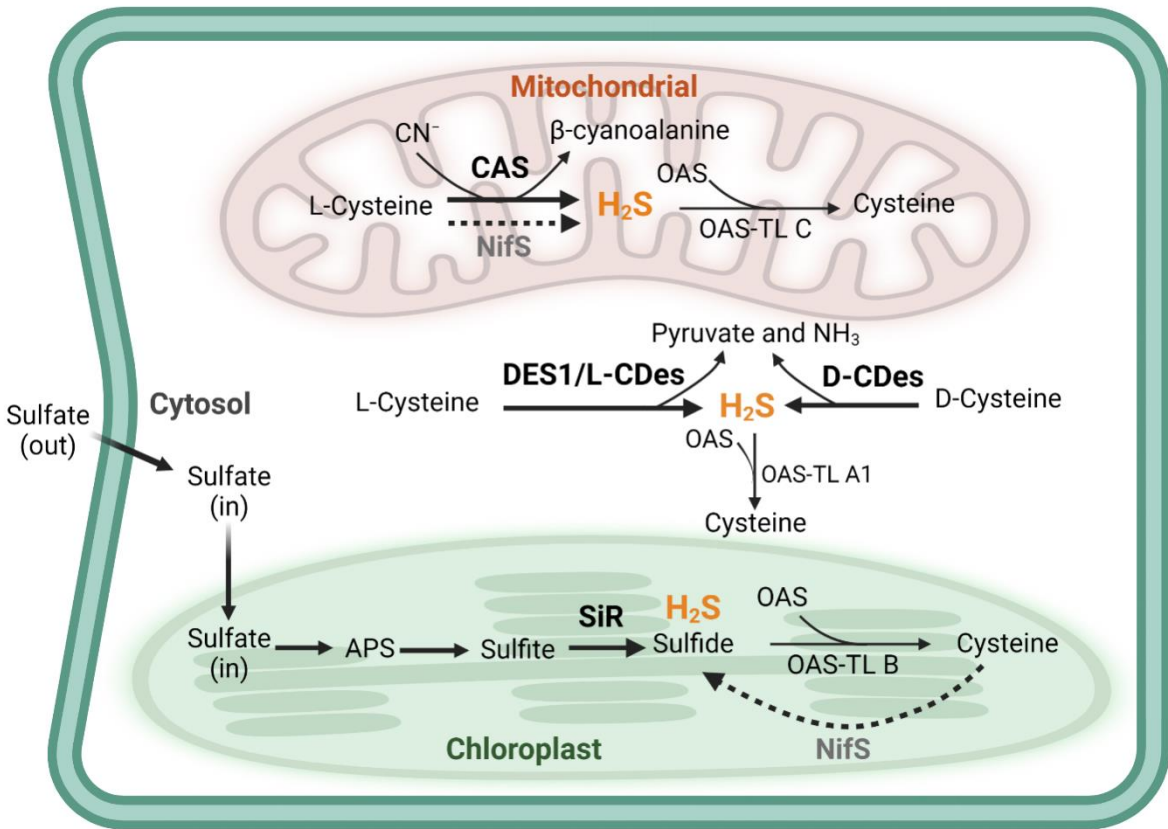


1251

1252

1253 **Fig. 1.**

1254

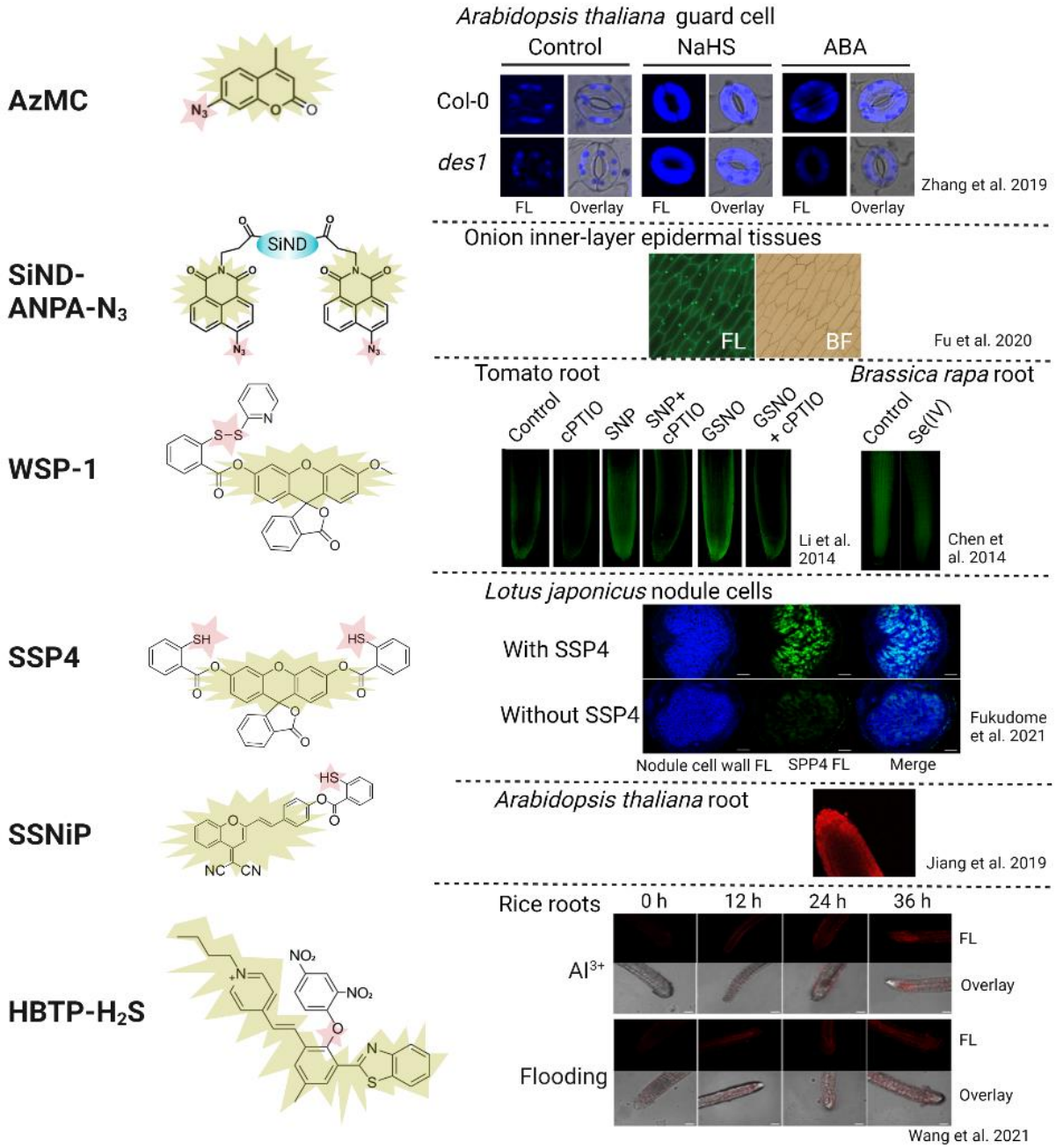


1255

1256

1257 **Fig. 2.**

1258

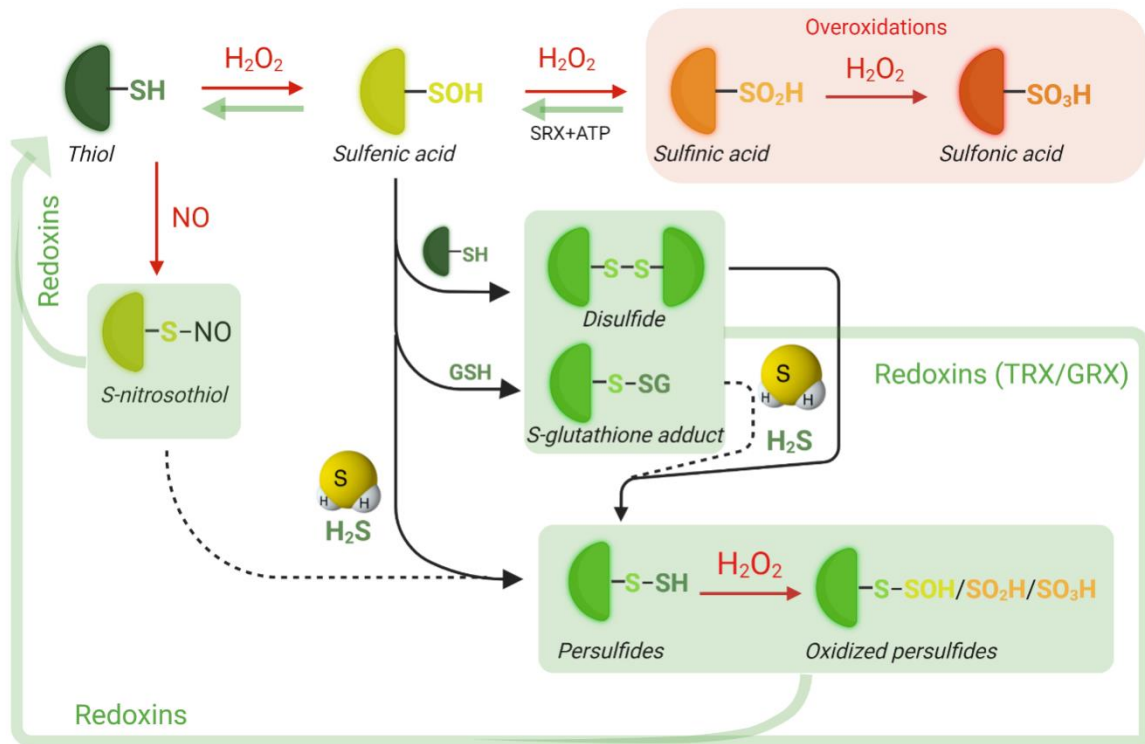


1259

1260

1261 **Fig. 3.**

1262

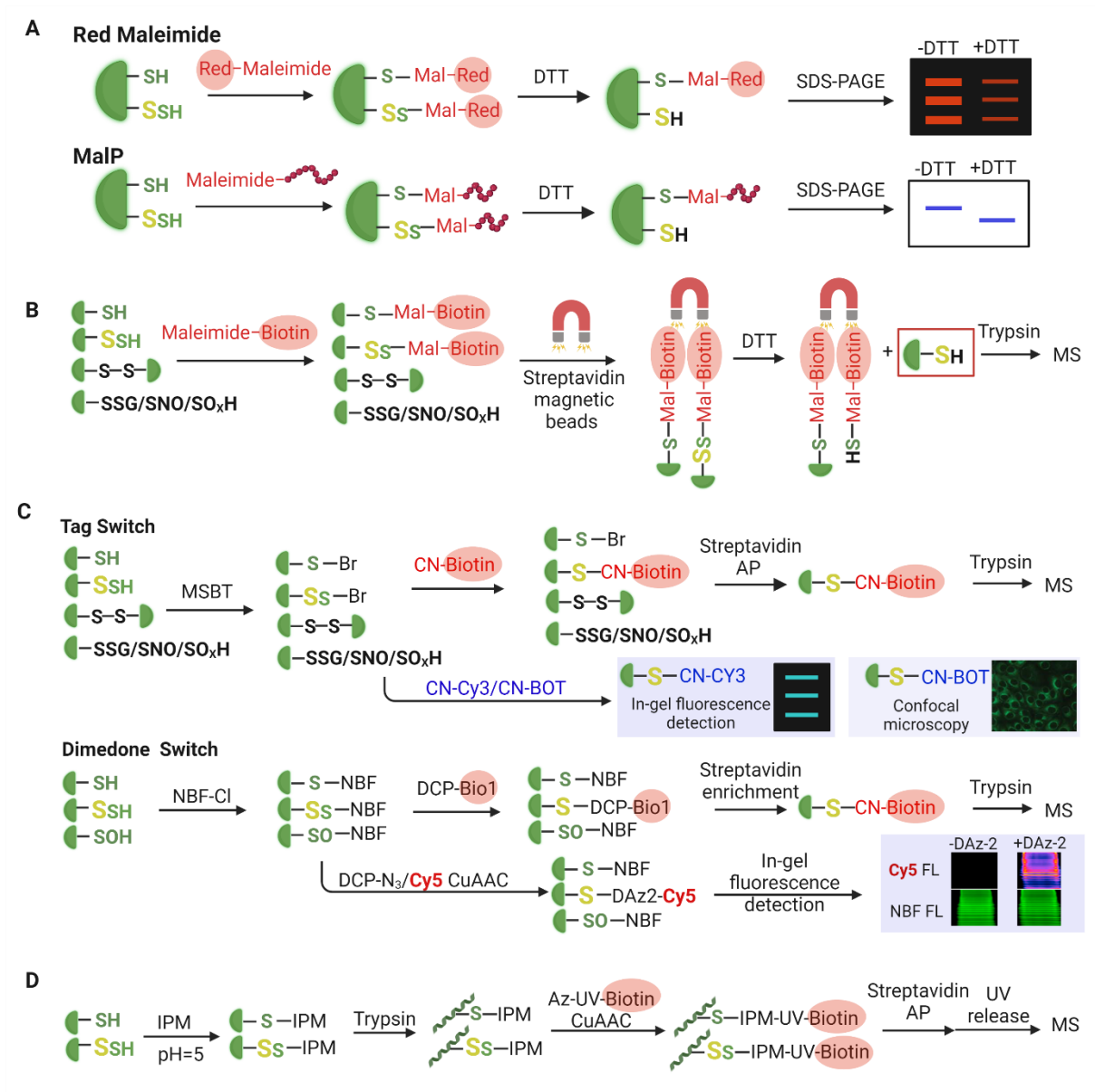


1263

1264

1265 **Fig. 4.**

1266

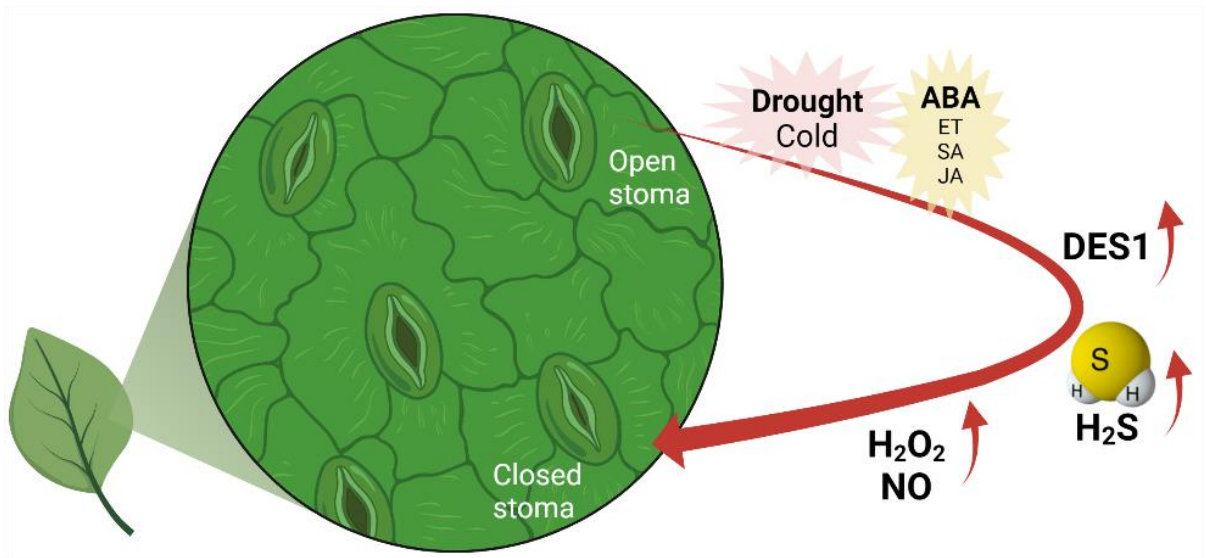


1267

1268

1269 **Fig. 5.**

1270

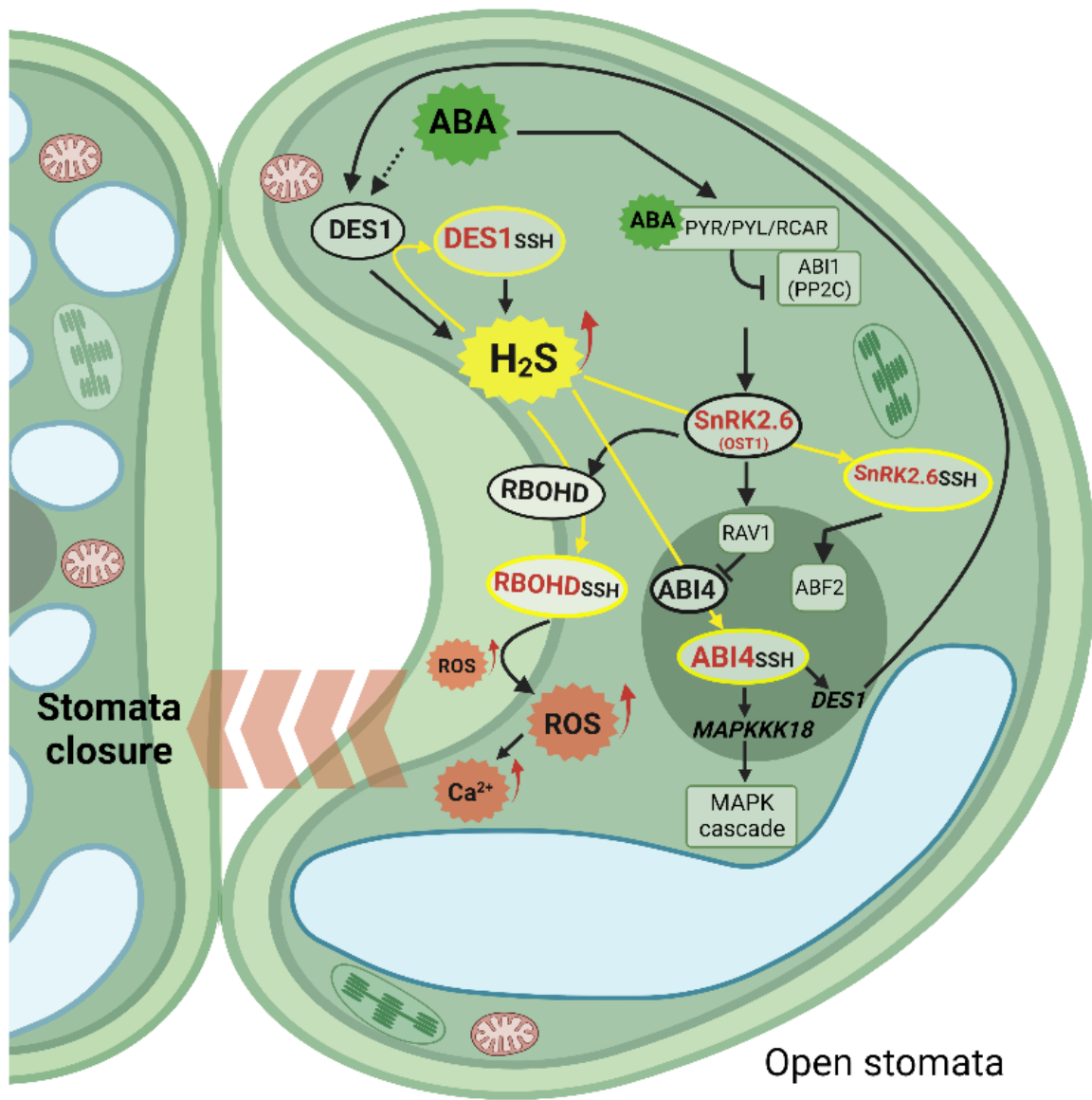


1271

1272

1273 **Fig. 6.**

1274



1275

1276

1277 **Fig. 7.**